MONTREAL PROTOCOL ON SUBSTANCES THAT DEPLETE THE OZONE LAYER

REPORT OF THE SCIENTIFIC ASSESSMENT PANEL

SEPTEMBER 2024

RESPONSE TO DECISION XXXV/7: EMISSIONS OF HFC-23

UN environment programme

15 September 2024*

Report of the Scientific Assessment Panel in response to Decision XXXV/7: Emissions of HFC-23

Lead Authors:

S. A. Montzka, NOAA Global Monitoring Laboratory, USA;
J. B. Burkholder, NOAA Chemical Sciences Laboratory, USA

Authors:

Co-Chairs of the Montreal Protocol Scientific Assessment Panel:
L. J. Carpenter, University of York, UK;
D. W. Fahey, NOAA Chemical Sciences Laboratory, USA;
K. W. Jucks, NASA Earth Science Program, USA;
B. Safari, University of Rwanda, Rwanda

Contributors:

Members of the Advanced Global Atmospheric Gases Experiment (AGAGE) Global Network;
L. Western, University of Bristol, UK;
K. M. Stanley, University of Bristol, UK;
A. J. Manning, UK Met Office, UK;
M. K. Vollmer, Swiss Federal Laboratories for Materials Science and Technology (EMPA), Switzerland;
M. Sulbaek Andersen, California State University, Northridge, USA

* Re-issued on 30 September 2024 for technical reasons.

Table of Contents:

Executive Summary:

From 2019 to 2022, the global mean atmospheric abundance of hydrofluorocarbon-23 (HFC-23; CHF_3) increased at Earth's surface by 1.13 ppt yr^{-1}. This rate of increase was 6% slower than the 1.20 ppt yr^{-1} observed during 2016-2020. HFC-23 atmospheric mole fraction reached 35.9 ± 0.9 ppt in 2022, accounting for 6.9 mW m^{-2} of radiative forcing. Total radiative forcing from all HFCs amounted to 44.1 mW m^{-2} in 2020.

Global emissions of HFC-23 estimated from measured atmospheric abundances have steadily decreased from a high of 17.3 ± 0.8 kt in 2019 (254 $MMTCO_2e$) to 13.9 ± 0.7 kt in 2022 (204 $MMTCO_2e$) in 2022. This decrease in emissions was observed despite an increase in total production of hydrochlorofluorocarbon-22 (HCFC-22; CHF_2Cl) reported for all uses from 2019 to 2022, noting that the principal source of HFC-23 is as a by-product from HCFC-22 production. The decline in global HFC-23 emissions while HCFC-22 production was increasing may reflect increased mitigation of HFC-23 emissions as an increasing number of parties ratified the 2016 Kigali Amendment to the Montreal Protocol.

Global emissions of HFC-23 estimated from measured atmospheric abundances can be contrasted with values derived from reporting to the United Nations Framework Convention on Climate Change (UNFCCC), the Multilateral Fund for the Implementation of the Montreal Protocol (MLF), and the Ozone Secretariat. From 1995 to 2014, good consistency was observed between estimated and reporting-based global emissions of HFC-23. This was the case even from 2005 to 2014 when reported HFC-23 destruction, mostly in China and supported by the UNFCC's Clean Development Mechanism (CDM), peaked near 9 kt yr^{-1}. After 2014, differences (or gaps) emerged between estimated and reporting-based global emissions of HFC-23. The gaps grew to reach a peak of 15 kt in 2019 and have decreased in the three years since 2019 to reach approximately 10.5 - 12.5 kt in 2022.

The increasing emission gaps between 2015 and 2018 are similar in magnitude and coincident in time with the destroyed amounts of HFC-23 reported by China to the MLF, amounts that are consistent with the country's Hydrochlorofluorocarbon Production Phase-out Management Plan (HPPMP) agreement with the MLF Executive Committee.

The emission gaps after 2015 are substantially larger than can be explained by emissions from all known sources and reported abatements. An assessment by the Technology and Economic Assessment Panel (TEAP) estimates HFC-23 emissions from all known sources and reported abatements after 2020 to be in the range of 1.47 - 3.54 kt yr^{-1}, which is substantially smaller than the atmospherically-derived mean of 15 kt yr^{-1} during 2020 to 2022.

The decrease in the gaps after 2020 is concurrent with a declining ratio of global atmospherically-derived HFC-23 emissions relative to reported total HCFC-22 production (E_{23}/P_{22}), suggesting an increase in the inferred overall abatement of HFC-23 emissions.

HFC-23 is produced in the atmosphere from reactions that oxidize fluorinated gases present in the atmosphere. An upper limit to this source in 2022 is estimated to be 0.43 kt HFC-23 yr^{-1}, which accounts for less than 3.1% of global HFC-23 emissions in that year. This estimate is an upper limit, meaning that the actual value could be substantially smaller. The magnitude of this HFC-23 source is estimated using measured atmospheric abundances of relevant fluorinated gases, where available, and laboratory kinetic studies of the reactions that lead to HFC-23 production.

New atmospheric measurements have refined the quantification of HFC-23 emissions in some geographic regions. The sum of available regional emission estimates is less than the global total derived from atmospheric abundances in the remote atmosphere, indicating that not all regional sources are included to date. Indeed, atmosphere-based estimates are not available for all parties producing HCFC-22 in recent years. Estimates have become available based on atmospheric abundances measured at stations in and around China, and new estimates or updates are available from the United Kingdom, western Japan, Korea, The Netherlands, and portions of Europe.

From 2015 to 2019, regional HFC-23 emission estimates were derived for eastern China from atmospheric abundances measured at the Gosan, Korea, station. The emissions from eastern China increased during these years from 5.7 ± 0.3 to 9.5 ± 1 kt yr^{-1} despite reporting provided to the MLF showing that by 2018 more than 95% of the HFC-23 generated in China had been destroyed, stored, or used as feedstock. The derived geographical distribution of regional sources is broadly consistent with known locations of fluorochemical production facilities in China, including those producing HCFC-22. Since 2020, additional HFC-23 measurements made at multiple sites in China suggest continued emissions of HFC-23 during 2020-2023, in amounts from two different regions of 3.2 ± 0.9 and 6.7 ± 3.1 kt yr^{-1}, which are substantially larger than A7 emissions for controlled processes reported for all of China to the Ozone Secretariat (between 0.5 to 1.1 kt yr^{-1} during 2020-2022). Based on these studies, unreported emissions from China account for approximately 20 to 50% of the global emissions gap during 2015 to 2022.

Estimates of regional emissions of HFC-23 derived from measured atmospheric abundances have also become available during 2008 to 2021 for a number of countries other than China or portions of those countries (Australia, Belgium, Democratic People's Republic of Korea, France, Germany, Ireland, Japan, Luxembourg, Netherlands, Republic of Korea, and the United Kingdom). Summed emissions in recent years from these countries totals 0.75 kt yr^{-1}, which is 0.4 kt yr^{-1} higher than their reporting and not enough to explain a significant portion of the global emission gap. Together, HCFC-22 production in China and these other regions accounted for about 85% of reported HCFC-22 production in 2022. Atmospherically-derived HFC-23 emission estimates are not available in recent years for the countries that account for nearly all of the remaining HCFC-22 production reported during 2022: India, the United States, and the Russian Federation.

A substantial shortfall remains in the attribution of global emissions of HFC-23 to known sources or regions despite the new information provided in this Supplemental Report. The gap between reported emissions and those inferred from atmospheric abundances is not reconciled by considering all known sources. The sum of updated estimates of previously unrecognized or unaccounted sources as provided

by TEAP (TEAP, 2024) and the estimated production from the atmospheric oxidation of other fluorinated industrial gases could reduce the emissions gap by as much as 3 kt/yr^{-1}. However, regional studies conclude that emissions in recent years from regions of China are substantially larger than expected from China as a whole (by as much as 6 kt), and they account for a substantial fraction of the gap (18-55%). These emissions have not been reported or considered previously in a quantitative assessment of the global gap. In contrast, the total of regional emissions from 11 other countries in recent years are small relative to the gap (less than 4%). A regional-scale accounting of global emissions remains incomplete, as atmosphere-based estimates are not available from some regions of the world that are potentially significant sources of HFC-23 emission.

1 Introduction

Decision XXXV/7 from the Thirty-Fifth Meeting of Parties of the Montreal Protocol on Substances that Deplete the Ozone Layer, held in Nairobi, Kenya, in October 2023, addressed issues related to production and emissions to the atmosphere of HFC-23. In paragraph 1 of this decision, the parties requested the Scientific Assessment Panel to prepare a report to the Thirty-Sixth Meeting of the parties as follows:

To request the Scientific Assessment Panel to provide an update on HFC-23 emissions into the atmosphere and atmospheric concentrations to supplement the information in the 2022 quadrennial assessment report, including by reflecting any new information regarding atmospheric monitoring and atmospheric modeling, with its underlying methodology, including in quantifiable terms, with respect to such emissions, and taking into account information reported under paragraph 3 ter of Article 7 by all parties that manufacture Annex C, Group I and/or Annex F substances, and to prepare a report on the matter to the Thirty-Sixth Meeting of the parties to the Montreal Protocol;

The following report is the response to this request. The report updates the information and conclusions provided for HFC-23 in Chapter 2 of the 2022 UNEP/WMO Scientific Assessment of Ozone Depletion (Liang and Rigby *et al*., 2022; hereafter referred to as 2022 SAR). The authors of this report are grateful for the collaboration with members of the Advanced Global Atmospheric Gases Experiment (AGAGE) Global Network, which is a multinational atmospheric monitoring collaboration. AGAGE provided updated global HFC-23 atmospheric abundances (mole fractions) measured in the remote atmosphere and global emission estimates through 2022, which extends by 2 years the results that appeared in the 2022 SAR. The observation-derived estimates of global emissions are essential for evaluating global budgets of substances controlled under the Montreal Protocol. Emission estimates have also become available for a few geographic regions on the basis of surface abundances measured at locations that capture recent emissions from regions upwind.

Estimated global emissions by year are compared to bottom-up estimates derived from information reported to the United Nations Framework Convention on Climate Change (UNFCCC), the MLF, and the Ozone Secretariat. This report also considers other key terms in the global budget of HCF-23. The first is the reported destruction of HFC-23 associated with fluorochemical production, primarily of HCFC-22. The second is the photo-chemical production of HFC-23 in the atmosphere from reactions that oxidize

fluorinated gases present in the atmosphere. This report provides an upper limit to this source that has not been available previously. Third, the combined source of HFC-23 in processes other than the production of HCFC-22 has been provided in the Report of the Technology and Economic Assessment Panel in response to Decision XXXV/7 (TEAP, 2024). Finally, the report includes a brief tutorial on deriving emissions on global to regional scales from atmospheric abundance or concentration measurements (Box 1).

The authors acknowledge the important assistance and input from a number of additional people: a representative from the Multilateral Fund for the Implementation of the Montreal Protocol; members of the Technology and Economic Assessment Panel, particularly H. Tope; B. Adams and M. Rigby for sharing their preliminary analysis of HFC-23 abundances measured in recent years; I. Vimont for providing updated abundances for some of the HFCs measured by NOAA that appear in Table 2; S. Reimann; J. Muhle; and a representative from the Ozone Secretariat for prompt and informative sharing of updated quantities associated with Montreal Protocol A7 reporting.

2 Background of the report

Chapter 2 of the 2022 UNEP/WMO Scientific Assessment of Ozone Depletion (Liang and Rigby *et al*., 2022; hereafter referred to as 2022 SAR) addressed observations and analyses of hydrofluorocarbons (HFCs) in the atmosphere, including available information on abundances, emissions and consequences for the climate system. The results for HFC-23 are summarized below as background to this report.

The global mean atmospheric abundance measured for HFC-23 in 2020 (33.7 ± 0.9 ppt) made it the third-largest contributor to radiative forcing (RF) among all HFCs (15% in 2020). Global mean concentrations of HFC-23 increased during 2018-2019 at the highest rate (1.3 ppt yr^{-1}) recorded throughout the measurement record; the overall change between 2016 and 2020 was 17 ± 4% (a mean of 1.2 ppt yr^{-1}), which was faster than the increase from 2012 to 2016 (a mean of 1.0 ppt yr^{-1}), the period assessed in the 2018 Scientific Assessment Report (Montzka and Velders *et al*., 2018). Global total HFC-23 emissions peaked during 2019 (17.3 ± 0.8 kt) and averaged 16.5 ± 0.9 kt yr^{-1} (243 ± 12 MMt CO_2e yr^{-1}) during 2018-2020, making it the third-largest contributor (20%) to GWP-weighted emissions from HFCs. This relatively large contribution of HFC-23 to CO_2e emissions stems from its long lifetime (228 yr) and its large 100-yr GWP (14700) compared to other HFCs (Burkholder and Hodnebrog *et al*., 2022). Projections assuming constant HFC-23 emissions into the future suggested that "HFC-23 has the potential to cause about half of the climate forcing (30 mW m^{-2}) of all the other HFCs, combined, by 2100" (Daniel and Reimann *et al*., 2022).

Surface-based abundances and trends for HFC-23 discussed in the 2022 SAR were provided by the global-scale surface measurement network, the Advanced Global Atmospheric Gases Experiment (AGAGE; an update of Prinn *et al*., 2018 and Park *et al*., 2023). Continued atmospheric increases in the global atmospheric abundance of HFC-23 have been derived from satellite retrievals (Schmidt *et al*., 2024) and by upward-pointing FTIR instrumentation above sites in Japan and Antarctica (Takeda *et al*.,

2021), although abundances suggested from these light absorption methods are 15-20% lower than the surface-based estimates.

Because the dominant source of HFC-23 to the atmosphere has historically been associated with over-fluorination during the production of HCFC-22 (TEAP, 2023), the ratio of global HFC-23 emissions relative to HCFC-22 production (E_{23}/P_{22}) totals can supply information about overall mitigation or destruction rates for HFC-23 generated as by-product. Based on reported production of HCFC-22 through 2019 and global HFC-23 emissions, the 2022 SAR noted: "*The ratio of global HFC-23 emissions inferred from atmospheric observations to reported HCFC-22 production has increased between 2010 and 2019, despite reports of substantial new emissions abatement since 2015*." Other potential sources of HFC-23 emission to the atmosphere unrelated to its generation as a by-product during the production of HCFC-22 were discussed but not quantified.

Global emissions of HFC-23 derived from reporting to the UNFCCC from Annex 1 countries and information supplied to the UNFCCC/Kyoto Protocol's Clean Development Mechanism (CDM) and to the MLF for other countries were compared to emissions estimated from measured trends and abundances in the remote atmosphere (Simmonds *et al*., 2018; Stanley *et al*., 2020; Liang and Rigby *et al*., 2022). Those comparisons showed good agreement (within ± 2 kt yr^{-1}) from 1995 to 2012. This consistency implied a good understanding through 2012 of the processes leading to the formation and emission of HFC-23, and that the amounts of generated HFC-23 that were destroyed between 2006 and 2012 through CDM projects (up to ~50% of co-produced HFC-23 and ~9 kt yr^{-1} in a few years) were accurately reported and estimated.

In 2013 and 2014, reporting-based emissions were notably larger than estimated from remote-atmosphere abundance measurements, and this discrepancy was thought to have arisen from a lack of clarity in reported and assumed quantities (Liang and Rigby *et al*., 2022).

Starting in 2015, however, a large divergence emerged between estimates of global HFC-23 emissions based on reporting versus those derived from atmospheric measurements in remote areas, with emissions estimated from global atmospheric concentration trends being substantially larger. The unexplained HFC-23 emissions were 15 ± 0.7 kt in 2019, the last year reporting-based estimates were available for consideration in the 2022 SAR. The Executive Summary of the 2022 SAR noted *"a large gap in our current understanding of most HFC-23 emissions reaching the atmosphere*." There was the recognition that other sources could contribute HFC-23 emissions independent of direct generation as a by-product during the production of HCFC-22, but their magnitudes were not thoroughly assessed.

The divergence in expected *vs.* atmosphere-derived emissions coincided with substantial increases in reported destruction of generated HFC-23 by China under the country's HPPMP and China's internal national voluntary efforts. During much of this period China accounted for the majority of HCFC-22 production (64 - 68% during 2015-2018) and HFC-23 generated as a by-product (67 to 69% during 2015-2017) worldwide (UNEP, 2018a,b).

India also announced HFC-23 emission mitigation efforts in October of 2016, although its contributions to global HCFC-22 production (57 kt or 6.7%) and generation of HFC-23 as a byproduct during HCFC-22

production (1.675 kt of HFC-23 or 8.3%) (UNEP, 2018a) during in 2016 accounted for less than 10% of global total HCFC-22 production and, for generated HFC-23, were small relative to the difference in reporting-based and atmosphere-derived global emissions of HFC-23 in that year.

Given the gap in understanding of emissions reaching the atmosphere, the 2022 SAR also considered the available regional emission estimates of HFC-23 based on atmospheric abundance measurements downwind of potential source regions. Emissions estimated from abundances measured at a site in China, from a survey in India, and from the United Kingdom were discussed, but could not account for global total emissions derived from atmospheric measurements in remote areas, particularly after 2015 when the gap in our understanding of global emissions substantially grew.

3 Updated HFC-23 information

In this supplemental report to the 2022 SAR, atmospheric measurements of HFC-23 after 2020 are presented, and they allow for updated estimates of global mole fractions and global emissions of HFC-23 through 2022 (Section 3.1). These updated global emissions are compared to reported emissions or estimates derived from reporting of other quantities (generation and abatements), as they are available. A brief discussion of other known industrial sources of HFC-23 is also included, based on the recent analysis by TEAP (in Section 4.1 of TEAP, 2024). A number of recently published studies describing atmospheric abundance measurements at sites that enable regional emission estimates are also considered (Section 3.3). Those updates provide new information for HFC-23 emissions from Australia and countries in eastern Asia and Europe. Finally, the potential for fluorine-containing gases to provide a source of HFC-23 via their atmospheric oxidation by the hydroxyl radical and ozone is explored (Section 4). Fluorine-containing gases are identified that can yield HFC-23 via atmospheric oxidation processes, and upper limits to the source of HFC-23 from atmospheric oxidative processes are estimated for the present day. Note that we adopt the terminology of TEAP (2024), where *generated or generation* are defined as the total HFC-23 produced as a by-product, without taking into account any emissions abatement.

The direct effect of the Kigali Amendment on emission trends of HFC-23 was unlikely to have been substantial in 2020, the last year considered in the 2022 SAR. This is because parties who were accounting for the majority of generated and emitted HFC-23 had not yet ratified the Amendment at that time and so were not obligated to adhere to its controls on HFCs. As of September 2024, the 2016 Kigali Amendment has been ratified by 160 countries and, of particular relevance to emissions of HFC-23, by all parties reporting HCFC-22 production in 2022 (Table 1).

The Kigali Amendment specifies that:

"*Each Party manufacturing Annex C, Group I, or Annex F substances shall ensure that for the twelve-month period commencing on 1 January 2020, and in each twelve-month period thereafter, its emissions of Annex F, Group II substances generated in each production facility that manufactures Annex C, Group I, or Annex F substances are destroyed to the extent practicable using technology approved by the*

Montreal Protocol in the same twelve-month period" (UNTC, 2019). The Kigali Amendment text indicates that its controls apply starting on the 90th day after ratification of the Amendment by a country.

Table 1: Dates of ratification for countries producing 99% of all reported HCFC-22 in 2022:

Party	**date**
China	17 June 2021
European Union	27 Sep 2018
India	27 Sep 2021
Japan	18 Dec 2018
Russian Federation	3 Oct 2020
United States	31 Oct 2022

These ratifications brought controls on production, consumption, and by-product-related emissions of HFC-23 into the framework of mechanisms and obligations for reporting, ensuring compliance, and consequences in cases of non-compliance, *etc*., that already applied to other Montreal-Protocol-controlled substances (*e.g*., chlorofluorocarbons (CFCs), HCFCs, halons, etc.). As is true for other chemicals controlled by the Montreal Protocol, HFC production and consumption for dispersive uses are scheduled for phase down with multiple schedules by the Kigali Amendment. In the case of HFC-23, additional controls apply to by-product-related emissions, and these emission controls are not subject to country-specific phase-down schedules. The emission controls specified in this Amendment apply beginning in 2020 or upon ratification, or in some instances, after ratification.

3.1 Global scale HFC-23 concentrations, emissions, and reported quantities related to HCFC-22 production

Updated abundance measurements of HFC-23 in the remote atmosphere provided by AGAGE show a continued increase in its global surface concentration (Figure 1; an update of Prinn *et al*., 2018 and Park *et al*., 2023). In 2022, the global surface mean concentration reached 35.9 ± 0.9 ppt, which amounts to 6.9 mWm^{-2} of radiative forcing. While HFC-23 surface concentrations have increased throughout the entire measurement record (2007-mid-2023), the rate of increase has slowed recently. During 2019 to 2022 the concentration increase averaged 1.13 ppt yr^{-1}, or approximately 6% slower than the mean rate measured from 2016 to 2020 (1.20 ppt yr^{-1}). Concurrent with this slower increase in global mean concentration, the hemispheric difference also decreased from a peak in 2019 of 1.40 ppt to 1.02 ppt in 2022 (Figure 2). The ACE satellite retrievals also reveal an increase in atmospheric concentrations of HFC-23, but they are not further assessed here given their known interferences (Schmidt *et al*., 2024).

Global emissions of HFC-23 estimated from updated trends and abundance measured in the remote atmosphere were higher in 2019 at 17.3 kt yr^{-1} than in any other year in the available record (Figure 2). Since 2019, global emissions have substantially decreased, consistent with concentrations not increasing as rapidly and hemispheric differences becoming smaller since that year. HFC-23 global emission in 2022, the most recent year for which an estimate is available, was 13.9 ± 0.8 kt yr^{-1}, which is 20 ± 7 % (3.5 ± 1.1 kt) below the 2019 value. This decline is similar to the drop in global HFC-23 emissions that

occurred from 2006 to 2009 (4.7 ± 1.1 kt; from 14.3 to 9.6 kt yr^{-1}), which was when CDM-facilitated destruction of HFC-23 emissions occurred.

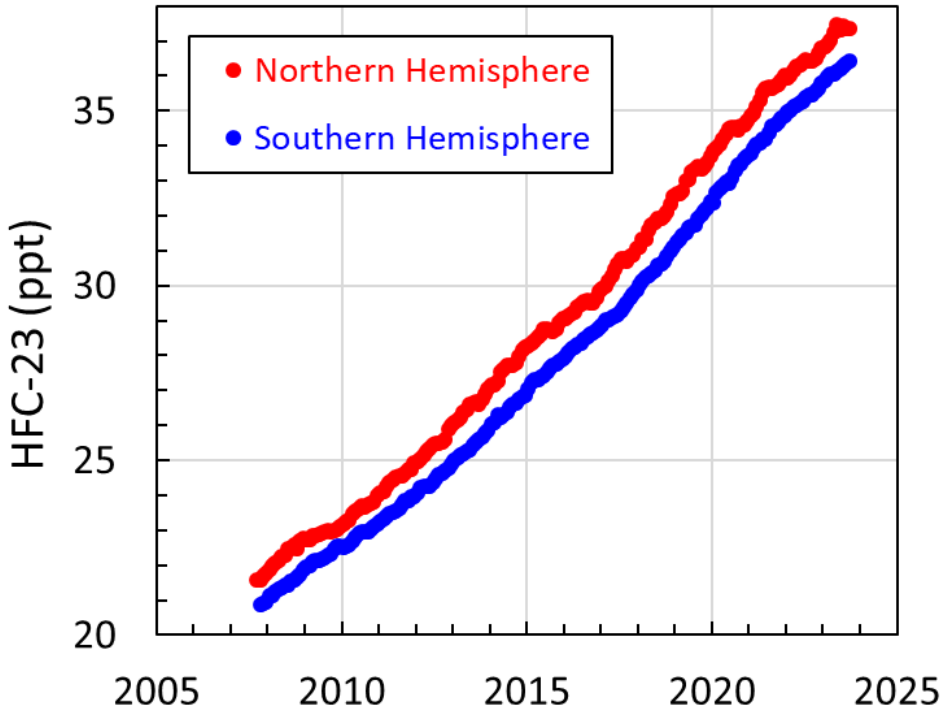

Figure 1: Atmospheric abundance of HFC-23 over time. *Monthly hemispheric surface means are estimated from measurements at remote sites by AGAGE (red = northern hemisphere; blue = southern hemisphere; an update of Prinn et al., 2018 and Park et al., 2023).*

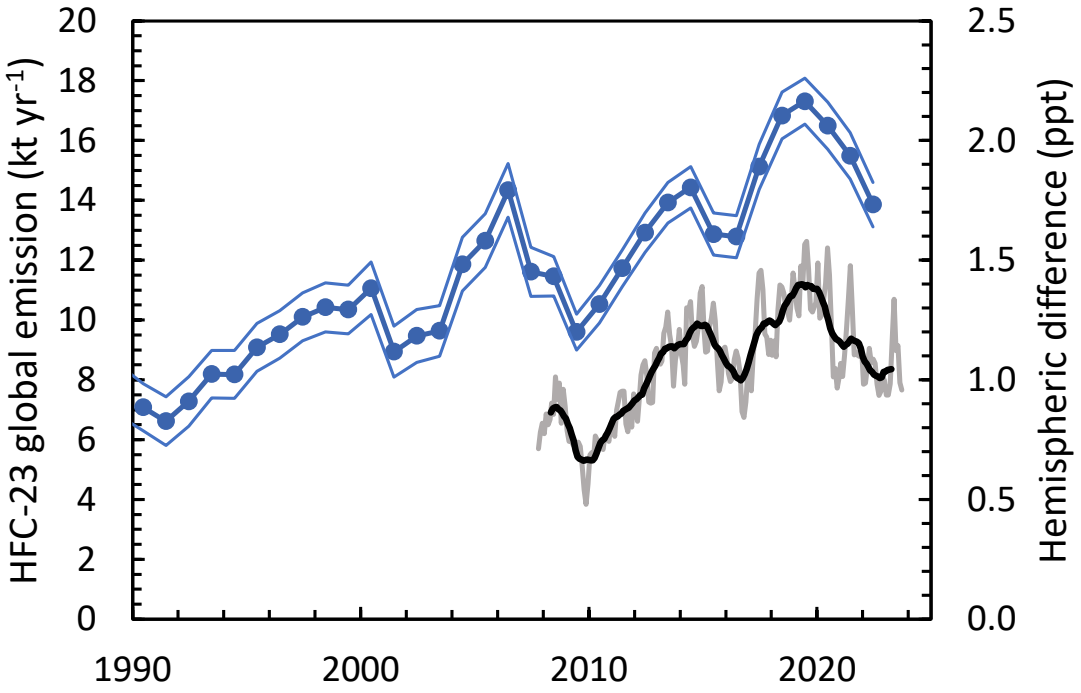

Figure 2. Global HFC-23 annual emissions and hemispheric concentration differences. *Global emissions (left-scale, blue points and lines) were estimated using established methods (12-box model) from measured concentrations and trends at remote sites by AGAGE (blue points connected by line, 1-sigma uncertainties are shown as lines; an update of Prinn et al., 2018 and Park et al., 2023). Hemispheric mean differences (right-hand scale; north minus south) are shown as 12-month running means (dark black line) and monthly differences (gray line) and are estimated from measurements at two to three sites in each hemisphere.*

The decline in global HFC-23 emissions from 2019 to 2022 was observed despite a concurrent and substantial increase in total reported production of HCFC-22 for all uses (17.5% from 2019 to 2022; 2022 global reported production was 1.2 MMt; Figure 3). The global increase in reported production from 2019 to 2022 stemmed predominantly from increasing feedstock production in A5 parties (+247.6 kt; while feedstock production in non-A5 parties increased 6.9 kt). Production for controlled uses has decreased since 2012 in both A5 and non-A5 parties. The COVID-SARS-2019 pandemic may have had an impact on global HCFC-22 production: total production in 2020 was approximately 10% lower compared to the mean in 2019 and 2021 for production in A5 parties; production in non-A5 parties dropped in 2020 and remained low in subsequent years.

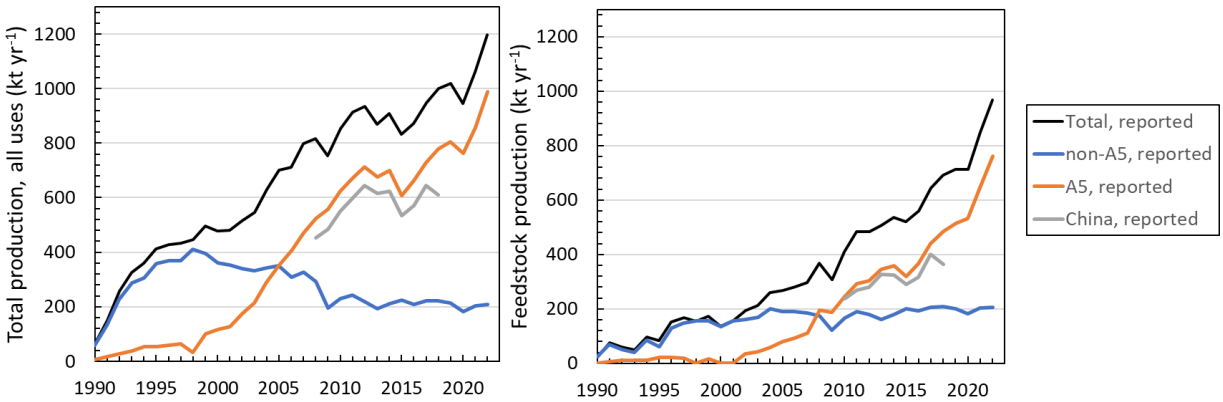

***Figure 3**: **Global reported production of HCFC-22**. Production of HCFC-22 reported to the Ozone Secretariat for all uses (left panel) and for only feedstock uses (right panel), legend applies to both panels. Total production (black lines) are broken out by contributions from A5 parties (tan lines) and non-A5 parties (blue lines), and from China (gray lines). Sources of China's totals: TEAP (2021, 2023); UNEP (2015).*

A main conclusion of the 2022 SAR related to HFC-23 and a substantial divergence between estimates of global HFC-23 emissions based on reporting versus those derived from atmospheric abundance measurements in remote areas (Liang and Rigby *et al*., 2022; Stanley *et al*., 2020). This divergence emerged in 2015 and remained substantial through 2019 (the last year data were available at that time), highlighting a substantial gap in our understanding of how and why global emissions have increased since 2015. This divergence followed a 20+ yr period when emissions estimated from remote-atmosphere concentration trends and reporting-based expectations (derived from emissions and CDM-related abatements reported to the UNFCCC, and information supplied to the Montreal Protocol's Ozone Secretariat) agreed to within ± 2 kt in all years (compare blue with solid-red lines in Figure 4). As part of this update, emission and abatement data reported to the UNFCCC (UNFCCC, 2024a; 2024b), the Ozone Secretariat (UNEP, 2024), and the MLF were reassessed through 2022, and the results confirm that these reporting-based emission expectations have been substantially lower than atmosphere-derived global emissions from 2015 through 2022 (Figure 4; compare blue and solid-red lines). This current report also resolved some double-counting issues in the reporting-based emissions and mitigation quantities during 2013 and 2014 that were apparent in an earlier analysis (Liang and Rigby *et al*., 2022).

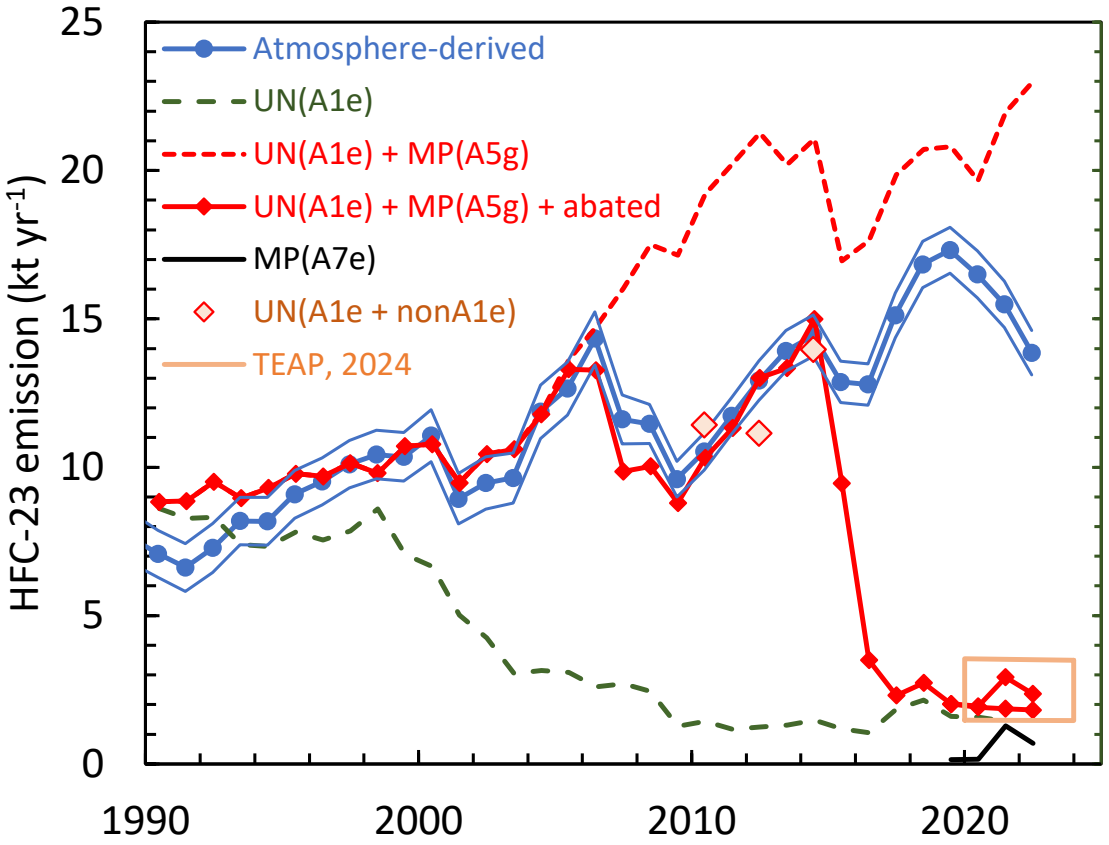

Figure 4; ***HFC-23 emissions over time****. Emissions estimated from atmospheric abundance measurements (blue lines with dots, with 1 s.d. uncertainty shown by surrounding thin lines) are compared to estimates derived from reporting of the sum of emissions from Annex 1 countries reported to the UNFCCC (UN(A1e); UNFCCC, 2024a) plus HFC-23 generated from A5 countries (MP(A5g)) minus abated (destroyed) amounts of generated HFC-23 during HCFC-22 production (this sum is hereafter called "expected" emissions; red solid line with diamonds). Also shown for reference: emissions reported from only Annex 1 countries to the UNFCCC (UN(A1e); UNFCCC, 2024a); dashed green line); those same Annex 1 UNFCCC emissions plus the sum total of HFC-23 generated during HCFC-22 production in A5 countries (MP(A5g); red dashed line; reported abatements not included; Stanley et al. (2020) through 2019 and from voluntary A7 reporting in 2020-2022); emission totals from A7 reporting to the Ozone Secretariat for reporting countries (MP(A7e); black line; UNEP, 2024); and the range of total emissions from all known industrial processes estimated by TEAP (tan-colored square, TEAP, 2024). In 2010, 2012, and 2014 the sum of UNFCCC net or actual emissions from all available countries are plotted (UN(A1e + nA1e); red diamonds with light-red fill; UNFCCC, 2024a, 2024b) and include emissions from only India and China in 2010 and only China in 2012 and 2014.* ***Notes****: UNFCCC emissions from Annex 1 countries in 2022 were unavailable and assumed to be equal to those in 2021 (UNFCCC, 2024a). The two values in 2021 and 2022 shown for expected emissions (red solid line with diamond symbols) reflect a difference in reporting by a single party in different publications (UNEP, 2022a).* ***Other sources****: Atmosphere-derived emissions: an update of Prinn et al. (2018), Liang and Rigby et al. (2022), and Park et al. (2023).*

Expected emissions that include abated quantities are estimated through 2012 as in the 2022 SAR and Stanley et al., (2020) and are based on reports under the UNFCCC CDM; after 2012, expected emissions are based on reported emissions, where available, or estimated emissions based on reported HCFC-22 production (for all uses) in the respective Article 5 countries, the assumed generation rates for HFC-23 by-production during HCFC-22 production (UNEP, 2018a;b), and information on HFC-23 management practices submitted by Article 5 countries.

The updated results show that emissions estimated from atmospheric measurements agreed within ± 2 kt yr^{-1} with expectations derived from reported emissions for the two decades preceding 2014 (Figure 4; compare blue and solid red lines). This agreement was observed during a period when a substantial decrease in emissions was reported from non-A5 countries, and when substantial destruction of HFC-23 was reported and verified through the UNFCCC's CDM projects, which were mostly in China (Figure 5). Starting in 2015, however, a difference between atmosphere-derived and reporting-based or expected global total emissions emerged and quickly grew; in 2015 it was 3 kt, in 2016 it was 9 kt, and from 2017 to 2020 it averaged 14.2 ± 1 kt yr^{-1}. By 2022, the gap magnitude had dropped slightly to 10.5 - 12.5 kt yr^{-1}. Considering A7 reported emissions would not have reduced the estimated value for the gap, since those emissions are even smaller than those being considered. The emergence of this difference, or "gap" in our understanding of emissions, in 2015, coincides with large increases in HFC-23 destruction quantities that were provided to the MLF by China that were consistent with the country's HPPMP agreement with the Executive Committee (Figure 5). Furthermore, the size of this difference during 2017 and 2018 is very similar to destruction magnitudes of HFC-23 inferred from reporting provided to the MLF by China during these years.

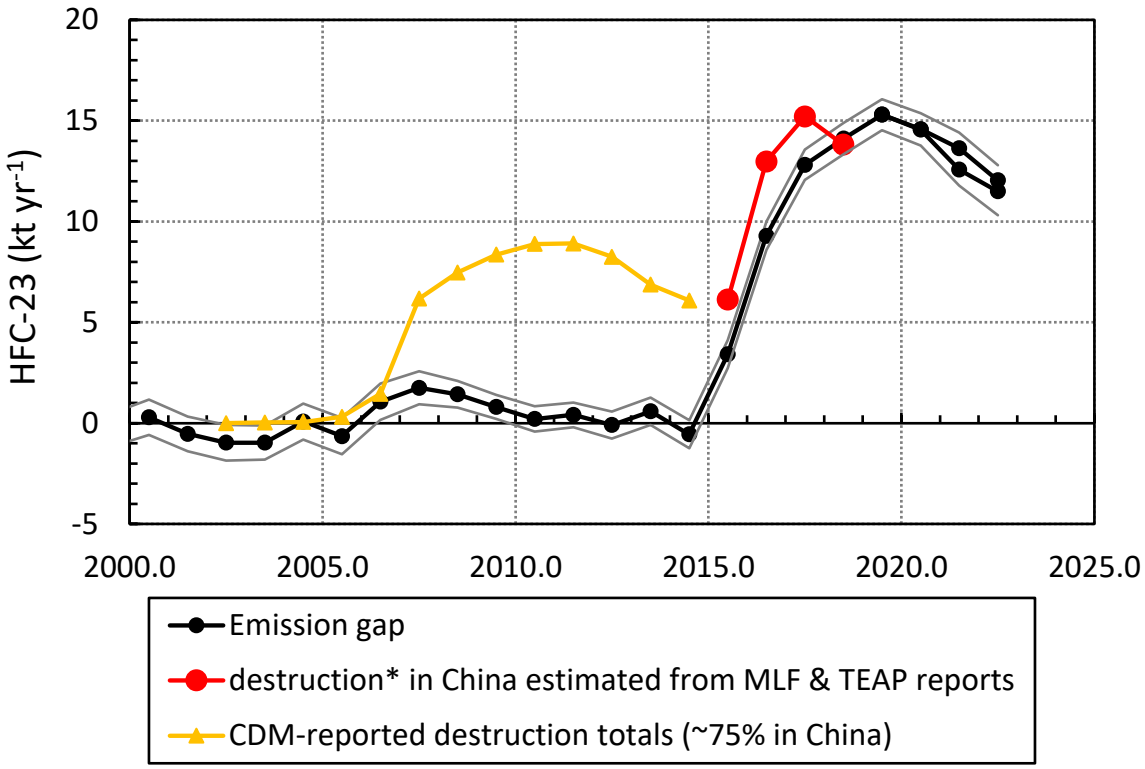

***Figure 5**. The difference between atmosphere-based and reporting-based estimates of HFC-23 emissions over time ("Emissions Gap", black lines with uncertainties associated with atmosphere-derived emission estimates). Also plotted are HFC-23 destruction amounts derived from reporting associated with CDM projects from all participating countries (yellow line; Stanley et al., 2020; with approximately 75% of the totals in most years being from destruction in China), and amounts of HFC-23 destroyed plus collection, storage, and sales reported by China (TEAP 2021, 2023), and reporting provided by China to the MLF for HFC-23 generation and HFC-23 destruction rates of 45, 93, 98, 99.8% in 2015-2018 (UNEP 2018a,b; UNEP, 2020; red line; destruction* = destroyed, collected, stored or sold). The destruction in 2018 (red open symbol) was estimated by assuming a HFC-23 generation rate from HCFC-22 production of 2.3% based on 2017, and a total reported HCFC-22 production reported in (TEAP, 2021). Two lines appearing in the "emissions gap" estimates after 2020 reflect some discrepancies in reported HFC-23 emissions (in China) in those years (UNEP, 2022a).*

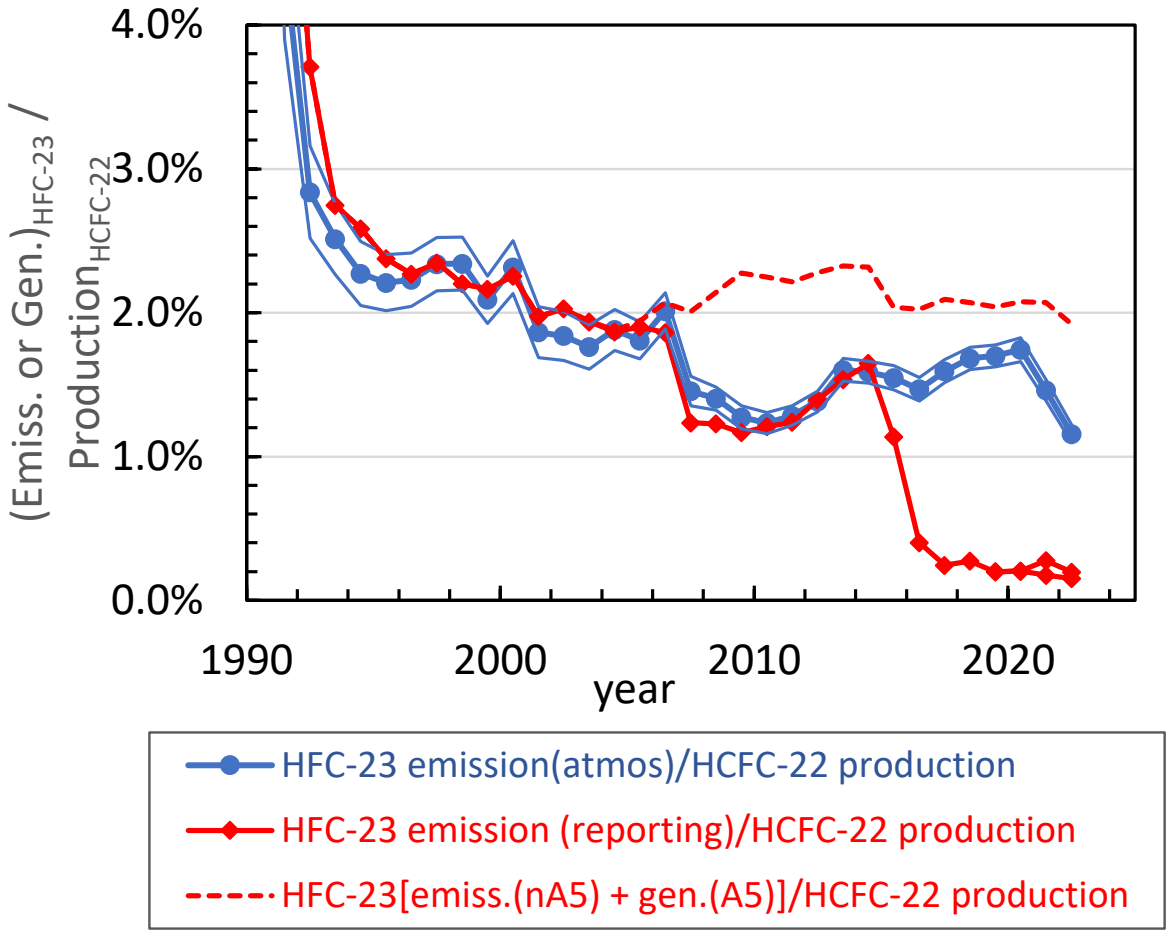

***Figure 6**: **Amounts of emitted or generated HFC-23 relative to reported HCFC-22 production**. Different estimates of HFC-23 emissions or emitted plus generated HFC-23 are plotted relative to total reported HCFC-22 production for all uses. HFC-23 emissions were estimated from atmospheric abundance measurements at remote sites (blue lines and dots, with 1 s.d. uncertainty shown by surrounding thin lines), and they were estimated from emissions reporting after subtractions associated with abated quantities as described in Figure 4 (red lines with diamonds). Also appearing is the sum of HFC-23 emissions from Annex 1 countries (UNFCCC, 2024a) plus HFC-23 generated in A5 countries without any subtractions to account for reported abatements (dashed red line here and in Figure 4). All three time series of emissions have been divided by total production of HCFC-22 reported to the Ozone Secretariat for all uses.*

The mean E_{23}/P_{22} derived for 2022 of ~1.16% is still larger than would be expected from the effective implementation of destruction technologies during the production of HCFC-22. For example, in MLF-funded projects, the term "to the extent practicable" corresponds to an E_{23}/P_{22} of 0.1% (UNEP, 2022b). The nominal overall E_{23}/P_{22} of 1.16% may be biased high by other sources or processes that create and release HFC-23 to the atmosphere, as described in Sections 3.2 and 4 of this report, and in Section 4.1 of TEAP (2024); the contribution of processes other than by-production during HCFC-22 production was estimated to be between 0.6 to 2.7 kt yr^{-1} of HFC-23 emission in recent years (TEAP, 2024). A recent

atmospheric-measurement-based study derived an E_{23}/P_{22} ratio of 0.19 (0.13-0.24) % for a fluorocarbon production facility in The Netherlands that produced HCFC-22 and monomers used to create polytetrafluoroethylene (PTFE; Rust *et al*., 2024), hence the HFC-23 emission detected may have included contributions from more than by-production during HCFC-22 production.

As highlighted in the 2022 SAR, the ratio of total HFC-23 emissions from all sources relative to HCFC-22 production for all uses (E_{23}/P_{22}) may be a useful metric for assessing the overall effectiveness of efforts to minimize HFC-23 emissions associated with HCFC-22 production (Figure 6). Through 2014, good consistency is observed for this ratio when emissions are estimated from reporting (red solid line with diamonds) or from atmospheric data (blue lines). This is true even during the CDM period from 2006 to 2014 when abatement reduced this ratio substantially below what it would have been in the absence of destruction (red dashed line). From 2015 to 2019, however, this E_{23}/P_{22} ratio increased on average, implying greater HFC-23 emission per amount of HCFC-22 produced. This is opposite to the expectations based on reporting that indicate large increases in overall destruction through those years. Since 2020 there has been a significant drop in the E_{23}/P_{22} ratio, implying that a smaller fraction of HFC-23 generated from HCFC-22 production has been released to the atmosphere. This decrease, from 1.74% to 1.16%, is slightly smaller than the decrease estimated during 2006 to 2009 (from 2.0% to 1.27%), which is likely associated with CDM-related abatements of HFC-23 by-product from HCFC-22 production.

3.2 HFC-23 emissions from all industrial processes

TEAP (2023, 2024) assessed all known industrial processes likely to contribute emissions of HFC-23 to the atmosphere and have estimated their magnitudes. Example processes include feedstock use, use as a fire suppressant, use in very cold temperature refrigeration, use as an etchant and cleaning agent in semiconductor and electronics manufacturing, and as a by-product from the production of HCFC-22, some HFCs, and chemicals created in the polymerization of HCFC-22 to produce plastics (*e.g.*, trifluoroethylene and hexafluoropropene). TEAP used a combination of reported and best-available information to estimate global HFC-23 emissions from all known sources to be between 1.47 and 3.54 kt yr^{-1} for the years 2020 to 2024 (see tan box in Figure 5), with between 0.6 and 2.7 kt yr^{-1} coming from processes other than by-production of HFC-23 during HCFC-22 production (TEAP, 2024). While some of the sources included in TEAP's estimate are accounted for by existing reporting to UNFCCC, for example, TEAP's analysis indicates that these other processes are not likely to explain more than a 2.7 kt of the 10.5 to 12.5 kt yr^{-1} gap during 2020-2022 (Section 3.1). Similarly, including the upper-limit to the atmospheric generation of HFC-23 from the oxidation of fluorinated gases (0.43 kt yr^{-1}, Section 4.0) explains only a small portion of the global emission gap.

Box 1: On methods used to derive emissions of long-lived gases like HFC-23 on global to regional scales from atmospheric abundance measurements.

This box describes the methods by which emissions of long-lived trace gases like HFC-23 on global and regional scales are estimated from atmospheric abundance measurements. The methods used in the

underlying atmospheric abundance measurements have not undergone substantial revision since the 2018 and 2022 SARs. For more detailed and quantitative descriptions, see the explanatory boxes in previous assessments (e.g., Laube and Tegtmeier et al., 2022).

***Estimates of global emission derived from atmospheric abundance measurements**.*

In this supplemental report, as in past Assessment reports, global emissions of long-lived trace gases are inferred using atmospheric measurements at a distribution of sites that allow for abundances (mole fractions or concentrations) to be measured in air that has not been impacted recently by emissions. For the purpose of estimating the sum of all emissions, the global measurement network is essential because it provides an accurate estimate of the global mean abundances of trace gases across Earth's surface and how those abundances change from year-to-year.

All long-lived trace gases controlled by the Montreal Protocol undergo photochemical or other reactions that lead to their chemical alteration and ultimate removal from the atmosphere. By considering all of these removal processes, a global loss frequency of the trace gas (units of % yr^{-1}) can be estimated along with the trace gas atmospheric lifetime (units of year) as the inverse of this global loss frequency.

A change in the global mean atmospheric abundance of a trace gas from year-to-year is a measure of the imbalance between cumulative sources (emissions) and cumulative losses (removal) of the gas:

Abundance change, per year = yearly emissions − yearly losses

To a good approximation, the yearly loss of a long-lived trace gas can be simply expressed as the global atmospheric abundance of the trace gas divided by its lifetime. Hence, yearly losses (as moles or grams removed per year) are directly proportional to the abundance of the trace gas. This approximation has several implications: first, in the absence of any source or emission of a trace gas, its global mean abundance will decline at a rate (% yr^{-1}) that is determined and limited by the lifetime of the trace gas. For example, in the absence of any emissions, the CFC-11 abundance would decline at approximately 2% per year given its global lifetime of about 50 yr, and HFC-23 would decline at 0.4% yr^{-1} given its global lifetime of 228 years. Second, it is not unusual for the global mean abundance of a trace gas to be increasing on an annual basis while its emissions are decreasing. This situation, as noted since 2019 for HFC-23 (Figures 1, 2), is understood as declining annual emissions that still remain larger than yearly losses. Hence, the balance of these terms has remained positive for HFC-23 since 2019, and its global mean abundance continues to increase.

A simple rearrangement of the equation above and substituting "(abundance/lifetime)" for loss gives the following relationship for a long-lived trace gas:

Yearly emissions = (Yearly abundance change) + (Average yearly abundance / atmospheric lifetime)

Thus, global annual emissions can be estimated from measured global trace-gas abundances and their annual changes, provided the atmospheric lifetime is known. Note that for HFC-23, with an average abundance change during 2019-2020 of 3.9% yr^{-1} (Liang and Rigby et al., 2022), its annual emission estimate is dominated by the measured abundance change and not loss, since the loss term is

substantially smaller (-0.4% yr^{-1}). This relationship applies to estimating emissions of trace gases having long lifetimes (greater than a few years). For shorter-lived gases, estimates of average yearly abundances and losses become more uncertain and, hence, estimated emissions become more uncertain.

Estimates of emissions on regional scales from atmospheric abundance measurements.

Emissions can be estimated on regional scales from atmospheric measurements if the measurement site is located downwind of the emission region of interest and if the emission sources are sufficiently large to cause enhancements above background values in the abundances measured at the site.

In recent publications considered in this Supplemental Report, two approaches have been used to derive regional HFC-23 emissions from atmospheric measurements made downwind of and near a source region. The first, interspecies correlation (ISC), relies on coincident measurements of a second trace gas whose regional emissions are thought to be better known than those of the primary gas for which emissions are being estimated. In these recent publications, emissions of HFC-23 are derived by measuring co-variations between HFC-23 and CO (carbon monoxide), HCFC-22, and PFC-318.

Uncertainties in regional emissions of HFC-23 using the ISC method stem from uncertainties in the emission estimates for the co-measured gases. They also stem from the fact that the two or more gases under consideration do not necessarily have co-located regional sources and similar temporal variability in emissions, with the result being that atmospheric transport and dilution processes affect the gases differently as they are transported from the source to the measurement site. These differences lead to more uncertainty in the emission estimates and can be assessed, in part, by the correlation coefficients determined from the timeseries of measured abundances of the gases.

The second approach is a regional flux inversion. This method was used in recently published work for estimating HFC-23 emissions on regional scales. These inversions require a simulation of transport of the trace gas from source locations to the downwind measurement site. Detailed meteorological information is required along with a statistical framework to relate the location and magnitude of the emissions to the enhanced abundances measured at the downwind site. Regions where meteorological data is reliable and the terrain between the sources and measurement site is simple (e.g. non-mountainous areas) yield the most accurate estimates of emission magnitudes and distributions with this approach.

In contrast to global estimates of emissions for long-lived trace gases, regional estimates of emission derived from regional flux inversions are insensitive to uncertainties in the trace gas lifetime. Instead, significant uncertainties arise in the inversion method from the need for accuracy in simulating atmospheric transport between the source region to the downwind site.

3.3 Regional contributions to global HFC-23 emissions

Further understanding of the underlying causes for unusual or unexpected global emission magnitudes and trends of controlled gases may be possible through consideration of emissions on country-wide or regional scales. This was apparent in the case of the unexpected increase in global emissions of CFC-11 that occurred after global production for dispersive uses had been phased out (*Montzka et al., 2018; Rigby et al., 2019; Chipperfield et al., 2021*). Since the 2022 SAR, studies have been published that provide estimates of HFC-23 emissions from a small number of countries. These results provide some insights, albeit incomplete, concerning regional contributions to ongoing HFC-23 emissions and how those emissions have changed over time from countries that account for about 85% of reported HCFC-22 production in recent years. Atmosphere-based emission estimates for HFC-23 do not always provide estimates that capture emissions from an entire country (*e.g.*, China and Japan), and they also are not currently available for all years through 2022. In addition, atmosphere-based estimates of HFC-23 emissions are not available in recent years (since 2016) for any countries or part of countries that account for most of the remaining global HCFC-22 production in 2022 (14% of the global total), and include India, the U.S.A., and the Russian Federation.

China has accounted for the largest amount of HFC-23 by-product generated in countries reporting production of HCFC-22. From 2013-2017, China accounted for 17.3 - 13.6 kt yr^{-1} HFC-23 (75-67% of global totals) (Table 2 in UNEP, 2018a,b; TEAP 2021); similar amounts of HFC-23 were generated by China in 2018 as 13.8 kt of HFC-23 were generated from the subset of HCFC-22 producing facilities receiving subsidies during that year (so not all HCFC-22 production in China; TEAP; 2021). Values in subsequent years are not currently available.

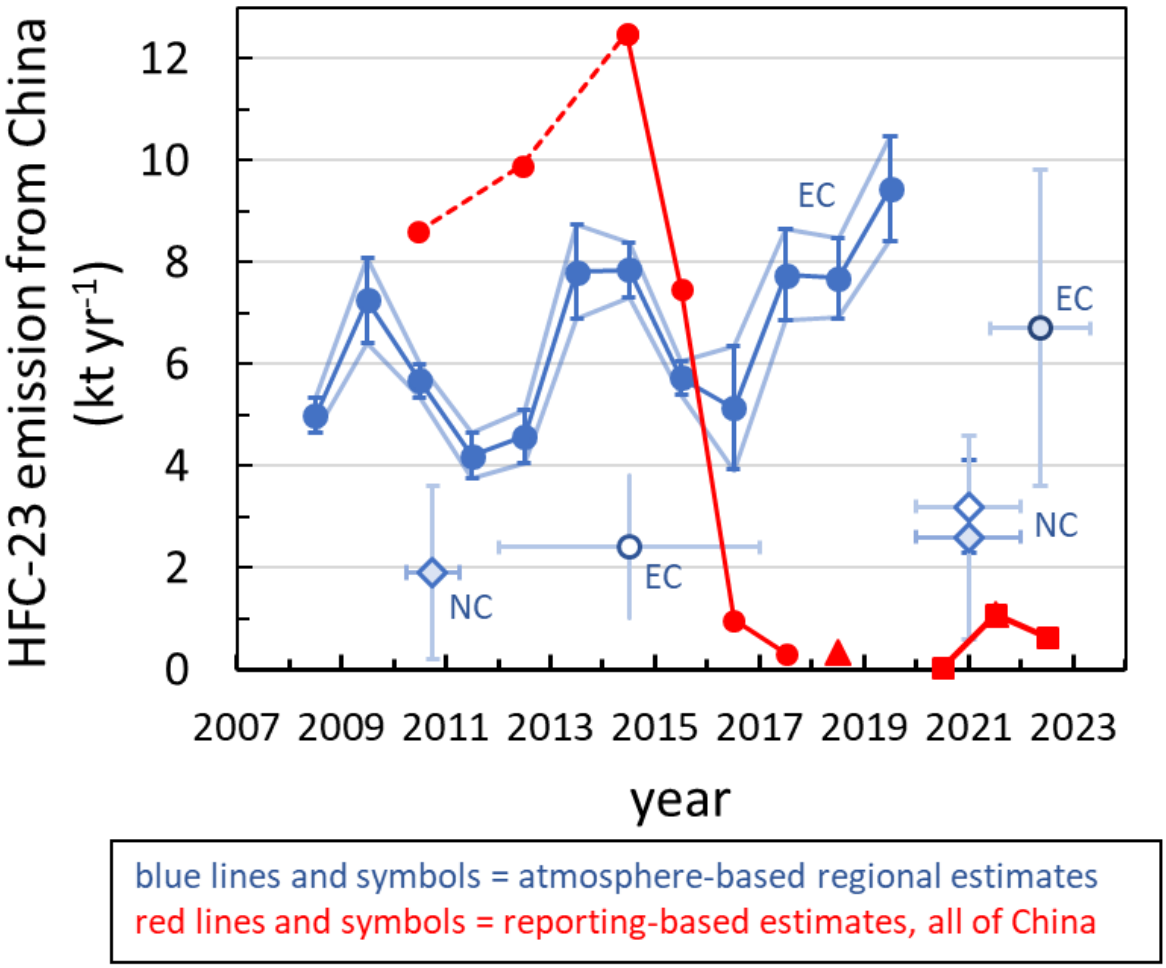

Figure 7. Atmosphere-based and reporting-based emissions of HFC-23 from China. *Emissions derived for different regions within China from atmospheric abundance measurements (blue lines and symbols; EC = eastern China, NC = northern China) are contrasted to emissions estimated for all of China from reports of emissions and abatements (red lines and symbols). Atmosphere-based estimates for these different regions cannot be combined to supply an estimate of emissions from all regions of China. Notes and sources: emissions from different portions of eastern China (EC) are derived from atmospheric measurements at Korea's Gosan Station (filled blue circles with 1-s.d. error bars; Park et al., 2023); from measurements at the Guangzhou Institute of Geochemistry (light-blue-filled blue circle using measurements from mid-2021 to mid-2023; Huang et al., 2024); and from measurements at the Lin'an regional station (Pu et al., 2020; white-filled blue circle labeled as EC*, measurements from mid-2012 through 2016). Emissions from northern China are derived from atmospheric measurements at the Shangdianzi Station (blue diamonds, derived using interspecies correlation with CO (light-blue filled diamonds in multiple years; Yao et al., 2012 in 2010-2011; and Yi et al., 2023 in 2020-2021) or HCFC-22 (white-filled diamond from 2020-2021) (Yi et al., 2023). Chinese total emission are shown a) for 2010, 2012, and 2014 based on reported "actual emissions" in category 2.E "production of halocarbons and SF_6" to the UNFCCC (red circles with dashed red line for these years only;*

https://di.unfccc.int/flex_non_annex1); b) for 2015-2017 based on reported generation as a by-product from HCFC-22 production and reported abated quantities (red line and solid circles; UNEP, 2018a,b; TEAP, 2021, 2023); c) for 2018 based on abated quantities for a fraction of total HCFC-22 production in China (red triangle; TEAP, 2021, 2023); and d) for 2020-2022 all of China based on A7 reporting of emissions to the Ozone Secretariat (red filled squares and lines; UNEP, 2024).

Newly published results and results considered in the 2022 SAR provide emission estimates of HFC-23 emissions for different regions over different periods of time, and are based on measurements at locations in northern China (Shangdianzi), southern China (Guangzhou Institute of Geochemistry), eastern China (Lin'an), and a Korean site downwind of China (Gosan) (Park *et al*., 2023; Pu *et al*., 2020; Yao *et al*., 2012; Huang *et al*., 2024; Yi *et al*., 2023). These studies suggest that emissions of HFC-23 from these different regions of China continued through the 2015-2023 period at rates in the individual regions that were larger that country-wide totals published as part of A7 reporting of HFC-23 emissions by China in 2020-2022, or that were derived for China in reports associated with the country's HPPMP agreement with the Executive Committee (UNEP, 2018a,b; UNEP, 2020).

From a high-frequency measurement record obtained at the Gosan station on Jeju island of the Republic of Korea (Park *et al*., 2023), emissions of HFC-23 and their distribution were also derived for other countries or portions of those countries in eastern Asia using an inverse-based analysis (see Methods box; Figure 7). Results indicate that eastern China dominated emissions from eastern Asia, with an average annual emission rate during 2008-2019 of about 7 kt yr^{-1}, varying between 4 to 10 kt yr^{-1}. From 2015 to 2019, estimated annual emissions from eastern China increased from 5.7 ± 0.3 to 9.5 ± 1.0 kt yr^{-1}, in sharp contrast to the substantial emission decrease expected on the basis of information concerning abatement magnitudes provided to the MLF during these years that were consistent with HPPMP agreements with the Executive Committee (red line in Figure 7). Regions estimated to have enhanced HFC-23 emission rates during 2015-2019 in this study corresponded to regions where most of the country's HCFC-22 reported production occurred in 2018 (TEAP, 2021), although some of China's HCFC-22 production facilities were located outside of the emission region well-characterized by measurements at the Korean GSN station. As a result, this study does not allow an estimate of China's total emission associated with generation as a by-product during HCFC-22 production or its total emission from all processes.

The HFC-23 emissions estimated for eastern China in Park *et al*. (2023) accounted for approximately 49 ± 11 % of global total emissions during 2008-2019 and the interannual changes in these Chinese emissions were highly correlated with those derived globally.

Emissions of HFC-23 from eastern China during 2012 to 2018 are substantially lower than estimated amounts of HFC-23 co-produced during these years, in part because of CDM-verified destruction between 2007-2014 (Figure 5), and because the atmosphere-derived emission estimates for eastern China most likely account for only a portion of China's total HFC-23 emission.

From a southern China site (GIG; Huang *et al*., 2024), a mean HFC-23 emission of 6.7 ± 3.1 kt yr^{-1} was estimated for eastern China using high-frequency measurements during mid-2021 to mid-2023,

providing measurement results for the period after China ratified the Kigali Amendment. The emissions were derived based on correlations with a second gas, PFC-318 (r = 0.74). The large (~50%) uncertainty associated with this emission estimate stems in part from the uncertainty associated with extrapolating the emission assumed for PFC-318 during these years (1.52 kt yr^{-1}) (see Box 1). Emissions for PFC-318 from all of China have recently been estimated (Wang *et al*., 2024) from flask measurements at 9 different sites distributed across the country. Those results spanned only through 2020, so prevent a definitive reassessment of the HFC-23 emissions derived in Huang *et al*. (2024) during mid-2021 to mid-2023.

Measurements of HFC-23 at a site in northern China (SDZ) were used to estimate emissions of 3.2 ± 0.9 (r = 0.51 vs HCFC-22) and 2.6 ± 2.0 kt yr^{-1} (r = 0.48 vs CO) for mid-2020 to mid-2021, also based on the ISC approach using HCFC-22 or CO (Yi *et al*., 2023). The HFC-23 estimate derived from measured covariations with HCFC-22 in this study are likely more reliable than those derived with carbon monoxide, owing to the larger uncertainties of the inventory emissions of CO compared to the inversion-based emissions of HCFC-22. While the authors estimate that the HCFC-22 emission they derived for northern China accounted for ~50% of China's total HCFC-22 emission, the fraction of China's total HFC-23 emission reflected in their atmosphere-based estimates is not known.

While the most recent results (Huang *et al*., 2024 and Yi *et al*., 2023) provide emission estimates from sites in different regions of the country, those regions are not entirely distinct and this fact makes combining them to provide an emission estimate representative for all of China difficult. Both results suggest that HFC-23 emissions from China continued into 2022 at rates that are substantially higher than reporting-based estimates suggest (Figure 7). These three studies (Park *et al*., 2023; Huang *et al*., 2024; and Yi *et al*., 2023) suggest that emissions from eastern China accounted for between 30 and 50% of global emissions during 2015 - 2019, and during 2021 - 2022, and emissions from northern China accounted for approximately 20% of global emissions in 2021-2022. Furthermore, after subtracting China's emissions accounted for in the analysis of the global emission gap (related to HPPMP as reported to the MLF and in A7-reporting to the Ozone Secretariat (UNEP, 2024)) the results from these three studies indicate that unaccounted regional emissions from China have accounted for approximately 18 to 55% of the global emissions gap from 2015 to 2022.

These recent studies from Huang *et al*. (2024) and Yi *et al*. (2023) only provided data for one or two years, preventing a quantitative estimate of regional emission trends or differences before and after 2021, the year that China ratified the Kigali Amendment. Concentration enhancements between the two years of the study (mid-2021 to mid-2022 vs. mid-2022 to mid-2023) were similar, suggesting no large emission changes over these two years.

Both Huang *et al*. (2024) and Yi *et al*. (2023) found that among the many different fluorinated gases measured at both the northern and southern Chinese stations, the highest correlation in concentration variations measured for HFC-23 were vs PFC-318. The correlation between HFC-23 and PFC-318 was similar at both these sites (r = 0.74 at GIG in the south and 0.80 at SDZ in the north), which suggests that half to two-thirds of the concentration variations observed for HFC-23 match those measured for PFC-318. Strong correlations in measured concentrations such as these suggest that a common source or co-

located source is contributing to emissions of both gases, although they do not rule out significant contributions from other sources. In Wang *et al*. (2024), emission distributions and magnitudes of PFC-318 were estimated for all of China based on a network of flask measurements made at 9 different sites distributed across the country. They found that regions in China with high emissions of PFC-318 overlap "with areas densely populated with [PTFE] factories, implying that fluoropolymer factories are important sources of PFC-318 emissions in China." Given the high correlation observed for HFC-23 and PFC-318 in different regions of China (Huang *et al*., 2024 and Yi *et al*., 2023), this may also be true for HFC-23, although these results do not eliminate the potential for other sources to also contribute substantially to HFC-23 emissions in China, particularly since many different industries exist in these same regions. TEAP (2024) estimates that the contribution to HFC-23 emissions from industrial processes associated with PTFE production accounts for between 0.1 to 1 kt of HFC-23 on a global scale, suggesting that this source cannot account for all HFC-23 emissions derived from China. Furthermore, the manufacturing of PTFE predates the emergence of the emission gap in 2015 by many years.

Abundance measurements at the Gosan station from 2008 to 2019 were also used to estimate emissions of HFC-23 from nearby countries and portions of countries. Mean (and maximum) annual emission of HFC-23 emissions estimated during 2008 to 2019 were 0.008 ± 0.004 (< 0.01) kt from the Democratic People's Republic of Korea (DPRK), 0.22 ± 0.16 (< 0.043) kt yr^{-1} from the Republic of Korea (ROK), and 0.14 ± 0.92 (< 0.21) kt from western Japan. While the emissions estimated for the Korean peninsula are thought to be representative of those entire countries, the analysis only allowed for emissions to be reliably estimated from western Japan. This region of Japan includes only a portion of their facilities producing HCFC-22. All three of these countries have reported HCFC-22 production to the Ozone Secretariat during 2019-2022, but amounts reported are small fractions of global totals (< 0.1% for DPRK, < 1% for ROK, and 2-3% for Japan).

Additional regions where emission estimates have been provided since the 2022 SAR include the United Kingdom, The Netherlands, north-western Europe, and Australia. In the United Kingdom (UK), HFC-23 emissions ranged from 0.01 to 0.02 kt during 2008-2017 and had decreased to 0.003-0.001 kt during 2019-2021, though uncertainties are large. Inventory-derived emissions are small in all years since 2010 (<0.003 kt, through 2019) (UNFCCC, 2023). For the Netherlands, a short-duration measurement study estimated annual emissions of 0.047 (0.036-0.055) kt yr^{-1} from a single facility that accounted for nearly all of the country's HFC-23 emission in the national inventory, which suggested 0.017 kt yr^{-1} in the latest inventory year of 2021 (Rust *et al*., 2024). HFC-23 emissions from a region encompassing much of north-western Europe (including Ireland, The UK, France, Belgium, The Netherlands, Luxembourg, and Germany) were estimated to be <0.15 kt yr^{-1} in all years since 2013 (Manning *et al*., 2022). HFC-23 emissions were estimated to be <0.1 kt yr^{-1} from 2005 to 2019 in inventory-based accounting and in atmosphere-derived results derived for Australia (UNFCCC, 2024).

Summing emissions associated with these updated atmosphere-based results suggests a total emission of HFC-23 in 2019-2022 of 0.75 kt yr^{-1} (countries or portions of countries included in this estimate: Australia, Belgium, DPRK, France, Germany, Ireland, Japan, Luxembourg, Netherlands, ROK, and the UK). Considering emissions reported from these countries during these years (approximately 0.36 kt yr^{-1}, UNFCCC, 2024a, 2024b), the updated atmospheric data suggest unaccounted emissions from these

countries is small (approximately 0.4 kt yr^{-1}) relative to the emission gap of 10.5 to 12.5 kt yr^{-1} in recent years.

4.0 Photo-chemical production of HFC-23 in the atmosphere

Potential photo-chemical production of CHF_3 (HFC-23) in the atmosphere was discussed in the 2022 SAR (Liang and Rigby *et al*., 2022). The report focused on HFC-23 production from the UV photolysis of CF_3CHO (trifluoroacetaldehyde), which is produced in the atmospheric oxidation of some F-containing gases. The report cited the CF_3CHO UV photolysis studies of Chiappero *et al*. (2006) and Sulbaek Andersen and Nielsen (2022), which reported HFC-23 product yield ([HFC-23] formed/[CF_3CHO] lost) upper-limits at atmospheric pressure of <0.02 for 308 nm photolysis and <0.003 obtained using broadband photolysis, respectively. It is important to note that neither study detected HFC-23 as a product in the UV photolysis of CF_3CHO at wavelengths relevant for the troposphere; they were only able to report an upper-limit on the product yield of HFC-23 based on their measurement sensitivity. Because it was performed in a manner that was more sensitive to detecting production of HFC-23, the Sulbaek Andersen and Nielsen study provides the best upper-limit to the product yield for use in interpreting the atmospheric production of HFC-23. There have been no additional peer-reviewed experimental studies of CF_3CHO photolysis under conditions relevant to the troposphere published since the 2022 SAR. The 2022 SAR indicated that atmospheric degradation of HFC-143a (CH_3CF_3), HFO-1234ze(E) ((*E*)-$CHF=CHCF_3$), and HCFO-1233zd(E) ((*E*)-$CF_3CH=CHCl$) could lead to the formation of CF_3CHO. A quantitative evaluation of the impact of this chemical/photochemical source of HFC-23 was not thoroughly investigated.

A comprehensive list of the source gases listed in the Annex of the 2022 SAR (Burkholder and Hodnebrog, 2022) having a chemical structure that could lead to the formation of HFC-23 in the atmosphere is given in Table 2. Saturated source gases having the CF_3CH_2– moiety will lead to the formation of CF_3CHO primarily via reaction with the OH radical through the CF_3CH_2O radical intermediate. The CF_3CH_2O radical rapidly reacts with O_2 in the atmosphere to form CF_3CHO:

$$CF_3CH_2O + O_2 \rightarrow CF_3CHO + HO_2$$

Unsaturated source gases (haloolefins) containing a $CF_3CH=$ moiety react with the OH radical to lead to the formation of CF_3CHO. These same unsaturated source gases can also react with ozone to produce HFC-23 directly (McGillen *et al*., 2023), but with small yields and at much slower rates than reaction with OH given typical ambient OH and ozone concentrations (see Table 2).

Not all CF_3CHO produced in the atmosphere results in HFC-23 production. CF_3CHO loss processes include UV photolysis, reaction with the OH radical, and deposition (wet and dry). The only pathway known to produce HFC-23 from atmospheric CF_3CHO is via UV photolysis, and only a very small fraction (<0.003) of the CF_3CHO removed by UV photolysis will produce HFC-23. The OH + CF_3CHO reaction will not lead to the formation of HFC-23, and deposition of CF_3CHO could lead to the heterogeneous formation of $CF_3C(O)OH$ (trifluoroacetic acid, TFA) (see Table 2 footnote). The estimated lifetime of CF_3CHO due to UV photolysis is ~4 days in the lower troposphere (Chiappero *et al*., 2006; Pérez-Peña *et al*., 2023), ~20 days due to reaction with the OH radical (k(298 K) = 5.7×10^{-13} cm^3 $molecule^{-1}$ s^{-1}) (Ammann *et al*., 2024), and wet/dry deposition is assumed here to have a ~7 day lifetime (Wallington *et al*., 1994). Considering these

losses, the total lifetime for CF_3CHO in the atmosphere is estimated to be ~2.2 days, with UV photolysis accounting for ~75% of CF_3CHO loss on a global scale as estimated by Pérez-Peña *et al*. (2023). Note that Sulbaek Andersen *et al*. (2023) have reported a CF_3CHO photolysis lifetime of 13 ± 4 days. For this report, the shorter photolysis lifetime of 4 days was adopted that provides a conservative upper-limit to the HFC-23 flux estimates presented below.

Table 2 includes estimates of atmospheric photochemical production rates of HFC-23 from source gas oxidation initiated by the OH radical and by ozone in the troposphere. These upper limit flux approximations for atmospheric production are derived from current atmospheric abundances of F-gases (global means for saturated HFCs and measured over Europe for HFOs), where available, reaction rate coefficients with OH and ozone assuming global mean [OH] of 1 x 10^6 radicals cm^{-3} and an ozone mixing ratio of 50 ppb, CF_3CHO production yields from chemical-specific degradation mechanisms, and the best currently available upper-limit to the HFC-23 product yield from atmospheric photolysis CF_3CHO (<0.003). Also included in the table are the relative contributions to HFC-23 production from F-gas oxidation by OH and the ozonolysis reaction pathway.

Table 2. Photochemical sources of CF_3CHO and HFC-23 (CHF_3) for species listed in the 2022 SAR Annex* (Burkholder and Hodnebrog, 2022) under conditions relevant for the global troposphere.

				OH reactive loss		O_3 reactive loss			
Name	Formula	Atmospheric Abundance	Global Lifetime (yr)	Tropospheric Lifetime [a] (yr)	CF_3CHO Product Yield [b] (%)	Tropospheric Lifetime [a] (yr)	CHF_3 Product Yield [c] (%)	Relative CHF_3 Yield: OH / O_3 Reactions [d]	Atmospheric CHF_3 Flux: OH Reaction / O_3 Reaction (kt/Yr)
Hydrofluorocarbons (HFCs)									
HFC-143a	CH_3CF_3	32 ppt (global)	51.8	57.2	100	$>1\times10^4$	ny	100 / –	<0.044 / –
HFC-236fa	$CF_3CH_2CF_3$	0.25 ppt (global)	213	253	100	nk	ny	100 / –	<0.0002 / –
HFC-245fa	$CF_3CH_2CHF_2$	3.75 ppt (global)	7.74	8.16	56	nk	ny	100 / –	<0.025 / –
HFC-365mfc	$CF_3CH_2CF_2CH_3$	1.1 ppt (global)	8.86	9.3	76	nk	ny	100 / –	<0.011 / –
Hydrochlorofluorocarbons (HCFCs)									
HCFC-133a	CH_2ClCF_3	0.45 ppt (global)	4.48	4.74	<5	nk	ny	100 / –	<0.0004 / –
HCFC-233fb	$CCl_3CH_2CF_3$	ud	16.4	29.3	100	nk	ny	100 / –	– / –
HCFC-234fb	$CCl_2FCH_2CF_3$	ud	37	97.8	<5	nk	ny	100 / –	– / –
HCFC-243fa	$CHCl_2CH_2CF_3$	ud	0.78	0.813	100	nk	ny	100 / –	– / –
HCFC-244fa	$CHFClCH_2CF_3$	ud	2.38	2.48	100	nk	ny	100 / –	– / –
HCFC-253fb	$CH_2ClCH_2CF_3$	ud	1.05	1.09	100	nk	ny	100 / –	– / –
Hydrofluoroolifins (HFOs)									
HFO-1243zf	$CH_2=CHCF_3$	ud	9 days	9 days	100	~1150 days	0.37 ± 0.02	98 / 2	– / –
HFO-1225zc	$CF_2=CHCF_3$	ud	2 days	2 days	100	nk	–	–	– / –
HFO-1234ze(E)	(*E*)-$CHF=CHCF_3$	0.15 (European)	19 days	19 days	100	~4600 day	3.11 ± 0.05	93 / 7	<0.15 / 0.009
HFO-1234ze(Z)	(*Z*)-$CHF=CHCF_3$	ud	10 days	10 days	100	~4600 days	–	–	– / –
HFO-1336mzz(E)	(*E*)-$CF_3CH=CHCF_3$	ud	122 days	122 days	200	~29000 days	–	–	– / –
HFO-1336mzz(Z)	(*Z*)-$CF_3CH=CHCF_3$	0.05 (European)	27 days	27 days	200	~19300 days	0.42 ± 0.02	99.9 / 0.1	<0.1 / 0.00009
HFO-1438mzz(E)	(*E*)-$CF_3CH=CHCF_2CF_3$	ud	122 days	122 days	100	nk	–	–	– / –
Hydrochlorofluoroolifins (HCFOs									
HCFO-1233zd(E)	(*E*)-$CF_3CH=CHCl$	0.15 ppt (European)	42.5 days	42.5 days	100	~8000 days	–	–	<0.09 / –
HCFO-1233zd(Z)	(*Z*)-$CF_3CH=CHCl$	ud		–	100	nk	–	–	– / –
									Totals: <0.42 / 0.009 kt/yr

Notes:

* Atmospheric abundances of saturated HFCs are global means updated for the end of 2023 (AGAGE; NOAA). Abundances indicated for HFOs are for abundances measures at the European Jungfraujoch site in 2020 or 2022 (Vollmer *et al*., 2015 updated in Liang and Rigby *et al*., 2022, and Rust *et al*., 2023). Given that global means for these short-lived HFOs are likely substantially lower than measured in Europe, the HFC-23 fluxes are also likely substantially lower than estimated here.

ud: Undetermined atmospheric abundance.

nk: No experimental rate coefficient measurements available. Lifetime and flux determination assume a rate coefficient of 1×10^{-24} cm^3 molecule^{-1} s^{-1} for the HFC and HCFCs and 1×10^{-22} cm^3 molecule^{-1} s^{-1} for the HFO and HCFO molecules (see footnote a).

ny: Ozone reactions with saturated HFCs and HCFCs are not expected to have any yield of CF_3CHO or CHF_3; CHF_3 product yields for ozone reactions with HFOs and HCFOs are not available; OH reactive lifetimes are taken from the Annex to the 2022 SAR (Burkholder and Hodnebrog, 2022).

The recent Salierno (2024) review proposes additional chemical pathways to the formation of CHF_3 through the heterogeneous chemistry of $CF_3C(O)OH$ (trifluoroacetic acid, TFA). However, no experimental evidence exists to suggest that this chemistry might actually occur in the atmosphere, making this suggestion speculative.

[a] Chemical lifetimes and HFC-23 fluxes were derived with reaction rate coefficients and [OH] = 1×10^6 radicals cm^{-3} and 50 ppb O_3.

Name	Formula	k(OH) (cm^3 molecule^{-1} s^{-1})	Reference	k(O_3) (cm^3 molecule^{-1} s^{-1})	Reference
HFC-143a	CH_3CF_3	1.3×10^{-15}	Burkholder et al. [2019]	$<3 \times 10^{-25}$	NIST
HFC-236fa	$CF_3CH_2CF_3$	3.3×10^{-16}	Burkholder et al. [2019]	– [a]	
HFC-245f	$CF_3CH_2CHF_2$	7.0×10^{-15}	Burkholder et al. [2019]	– [a]	
HFC-365mfc	$CF_3CH_2CF_2CH_3$	6.9×10^{-15}	Burkholder et al. [2019]	– [a]	
HCFC-133a	CH_2ClCF_3	1.2×10^{-14}	Burkholder et al. [2019]	– [a]	
HCFC-233fb	$CCl_2FCH_2CF_3$	1.28×10^{-15}	Papanastasiou et al.[2018]	– [a]	
HCFC-243fa	$CHCl_2CH_2CF_3$	4.6×10^{-14}	Papanastasiou et al.[2018]	– [a]	
HCFC-244fa	$CHFClCH_2CF_3$	1.51×10^{-14}	Papanastasiou et al.[2018]	– [a]	
HCFC-253fb	$CH_2ClCH_2CF_3$	3.45×10^{-14}	Papanastasiou et al.[2018]	– [a]	
HFO-1243zf	$CH_2{=}CHCF_3$	1.45×10^{-12}	Burkholder et al. [2019]	1.41×10^{-20}	McGillen et al. [2023]
HFO-1225zc	$CF_2{=}CHCF_3$	1×10^{-12} [a]	–	– [a]	
HFO-1234ze(E)	(*E*)-$CHF{=}CHCF_3$	7×10^{-13}	Burkholder et al. [2019]	2.44×10^{-21}	McGillen et al. [2023]
HFO-1234ze(Z)	(*Z*)-$CHF{=}CHCF_3$	1.35×10^{-13}	Burkholder et al. [2019]	$\sim 1.65 \times 10^{-21}$	Nilsson et al. [2009]
HFO-1336mzz(*E*)	(*E*)-$CF_3CH{=}CHCF_3$	1.3×10^{-13}	Burkholder et al. [2019]	4.14×10^{-22}	Østerstrøm et al. [2016]
HFO-1336mzz(*Z*)	(*Z*)-$CF_3CH{=}CHCF_3$	4.8×10^{-13}	Burkholder et al. [2019]	6.81×10^{-22}	McGillen et al. [2023]
HFO-1438mzz(E)	(*E*)-$CF_3CH{=}CHCF_2CF_3$	9.07×10^{-14}	NIST	$\sim 4 \times 10^{-22}$	NIST
HCFO-1233zd(E)	(*E*)-$CF_3CH{=}CHCl$	3.5×10^{-13}	Burkholder et al. [2019]	1.46×10^{-21}	NIST
HCFO-1233zd(Z)	(*Z*)-$CF_3CH{=}CHCl$	9.4×10^{-13}	Burkholder et al. [2019]	1.53×10^{-21}	Andersen et al. [2015]

[b] CF_3CHO product yields are taken from the literature for HFC-143a, HFC-245fa, and HFC-365mfc. In the absence of experimental data, CF_3CHO product yields are estimated using structure activity relationships for site specific reactivity (for HCFC-133a and HCFC-234fb atmospheric loss is not

expected to lead to the formation of CF_3CHO) or conservatively estimated to be nearly 100% based on reaction mechanisms for similar compounds.

[c] The HFC-23 yield in the ozonolysis reactions of saturated halocarbons is taken to be zero. The HFC-23 yield in the ozonolysis reactions of unsaturated haloolefins is taken from the literature where available.

[d] The relative yields (%) of HFC-23 from the OH reactive loss of the compound are calculated assuming a 0.003 yield of HFC-23 in the UV photolysis of CF_3CHO. Note that 0.003 represents an upper-limit for the HFC-23 product yield in CF_3CHO photolysis. A lower yield would result in less overall atmospheric production of HFC-23.

Overall, the annual total flux of HFC-23 estimated in Table 2 (<0.43 kt yr^{-1}, which is the sum of <0.42 kt yr^{-1} from OH reactions plus 0.009 kt yr^{-1} from ozonolysis reactions) is small relative to other sources discussed elsewhere in this report and the global emission "gap". These estimates are derived for the troposphere with our current understanding of the processes involved. They suggest that OH-initiated reactions dominate the HFC-23 production over production by ozonolysis. Reactive losses of the chemicals listed in Table 2 also occur in the stratosphere, but losses there typically account for only a small fraction of total losses. Different conditions present in the stratosphere (total pressure, temperature, UV flux, CF_3CHO photolysis lifetime, etc.) could affect overall yields and estimated production rates for HFC-23, but a lack of wavelength dependent and consistent pressure dependent CHF_3 product yield measurements (Chiappero *et al*., 2006 and Sulbaek Andersen *et al*., 2023) limits an evaluation of stratospheric CHF_3 production rates at this time. Perhaps the largest uncertainty in the fluxes derived in Table 2 stems from use of an upper limit to the CF_3CHO UV photolysis product yield of 0.003. If updated work were able to directly measure the product yield of HFC-23 in the photolysis of CF_3CHO, it likely would reduce the estimates of total HFC-23 flux in Table 2, while the absolute contribution from the ozonolysis reaction pathway of the unsaturated compounds would be unchanged.

Furthermore, the annual atmospheric production of HFC-23 from the oxidation of HFOs is likely to be lower on a global scale than the values in Table 2, given that global mean concentrations of these short-lived gases are very likely substantially smaller than those measured over Europe and used to derive the upper limits fluxes of HFC-23. More accurate estimates of HFC-23 atmospheric production in the oxidation of HFCs and HFOs await both the further refinement of the actual product yield of HFC-23 from the photolysis of CF_3CHO and a more sophisticated analysis of global-scale concentrations of HFOs and production in the stratosphere.

Pérez-Peña *et al*. (2023) have evaluated the contribution of CF_3CHO photolysis to the production of atmospheric HFC-23 using a box model that includes an evaluation of CF_3CHO atmospheric loss processes other than UV photolysis. The foam-blowing agent HFO-1234ze was used as the model source gas for the production of CF_3CHO in a hypothetical scenario that considered 12.6 kt yr^{-1} of HFO-1234ze emission, which was the global emission rate of the foam-blowing agent HCFC-141b in 2015 (although HFO-1234ze is not typically used in applications where HFC-141b was most often used). In a global model (Wang *et al*., 2021), this emission scenario yielded a global atmospheric concentration of HFO-1234ze substantially

higher (0.55 ppt globally) than currently measured in source regions (Europe, for example; Vollmer *et al*., 2015 and Liang & Rigby *et al*., 2022). Furthermore, the global flux of HFC-23 estimated from HFO-1234ze in that scenario (an amount accounting for 4% of the global growth rate of HFC-23) is likely too large by a factor of ~5 due to an apparent misinterpretation of results in Sulbaek Andersen *et al*. (2022).

5.0 References

Ammann, M., J. N. Crowley, H. Herrmann, M. E. Jenkin, V. F. McNeill, A. Mellouki, and J. Troe, IUPAC Kinetic Database, (2024), https://iupac.aeris-data.fr.

Andersen, L., F.F Østerstrøm, M.P. Sulbaek Andersen, O.J. Nielsen, and T.J. Wallington, Atmospheric chemistry of cis-CF3CH=CHCl (HCFO-1233zd(Z)): Kinetics of the gas-phase reactions with Cl atoms, OH radicals, and O_3, *Chem. Phys. Lett. 639*, 289–293 (2015), https://doi.org/10.1016/j.cplett.2015.09.008

Burkholder, J. B., S. P. Sander, J. Abbatt, J. R. Barker, C. Cappa, J. D. Crounse, T. S. Dibble, R. E. Huie, C. E. Kolb, M. J. Kurylo, V. L. Orkin, C. J. Percival, D. M. Wilmouth, and P. H. Wine (2019), "Chemical Kinetics and Photochemical Data for Use in Atmospheric Studies, Evaluation No. 19," JPL Publication 19-5, Jet Propulsion Laboratory, Pasadena (2020) http://jpldataeval.jpl.nasa.gov

Burkholder, J.B. and Ø. Hodnebrog, Annex: World Meteorological Organization (WMO). Scientific Assessment of Ozone Depletion: 2022, GAW Report No. 278, 509 pp.; WMO: Geneva (2022).

Chiappero, M. S., F. E. Malanca, G. A. Argüello, S. T. Wooldridge, M. D. Hurley, J. C. Ball, T. J. Wallington, R. L. Waterland, and R. C. Buck, Atmospheric chemistry of perfluoroaldehydes ($C_xF_{2x+1}CHO$) and fluorotelomer aldehydes ($C_xF_{2x+1}CH_2CHO$): Quantification of the important role of photolysis, *J. Phys. Chem. A*, *110*(43), 11944-11953, (2006) doi:10.1021/jp064262k.

Chipperfield, M., M.I. Hegglin, S.A. Montzka, P.A. Newman, S. Park, S. Reimann, M. Rigby, A. Stohl, G.J.M. Velders, H. Walter-Terrinoni, and B. Yao, *Report on the unexpected emissions of CFC-11*, World Meteorological Organization, rpt. no. 1268, ISBN 978-92-63-11268-2, Geneva, Switzerland (2021) [available at: https://ozone.unep.org/system/files/documents/SAP-2021-report-on-the-unexpected-emissions-of-CFC-11-1268_en.pdf]

Daniel, J. and S. Reimann (Lead Authors) *et al*., Chapter 7: World Meteorological Organization (WMO). Scientific Assessment of Ozone Depletion: 2022, GAW Report No. 278, 509 pp.; WMO: Geneva (2022).

Hu, L., S.A. Montzka, S.J. Lehman, D.S. Godwin, B.R. Miller, A.E. Andrews, K. Thoning, J.B. Miller, C. Sweeney, C. Siso, J.W. Elkins, B.D. Hall, D.J. Mondeel, D. Nance, T. Nehrkorn, M. Mountain, M.L. Fischer, S.C. Biraud, H. Chen, and P.P. Tans, Considerable contribution of the Montreal Protocol to declining greenhouse gas emissions from the United States, *Geophys. Res. Lett., 44* (15), 8075–8083 (2017) doi:10.1002/2017GL074388.

Huang, X., Y. Zhang, C. Xiao, W. Song, Y. Wang, and X. Wang, Constraining trifluoromethane (HFC-23) emission in eastern China based on two-year online measurements, *J. Geophys. Res. Atmos.*, *129*, e2023JD040199 (2024) https://doi.org/10.1029/2023JD040199.

Laube, J. and S. Tegtmeier (Lead Authors) *et al*., Chapter 1: World Meteorological Organization (WMO). Scientific Assessment of Ozone Depletion: 2022, GAW Report No. 278, 509 pp.; WMO: Geneva (2022).

Liang, Q., and M. Rigby (Lead Authors) *et al*., Chapter 2: World Meteorological Organization (WMO). Scientific Assessment of Ozone Depletion: 2022, GAW Report No. 278, 509 pp.; WMO: Geneva (2022).

Manning, A., S. O'Doherty, D. Young, Al. Redington, D. Say, J. Pitt, T. Arnold, C. Rennick, M. Rigby, A. Wisher, A. Wegner, and P. Simmonds, Long-term atmospheric measurements and interpretation of radiatively active trace gases, October 2020 - September 2021 (2022) https://assets.publishing.service.gov.uk/media/62d7b9bee90e071e7e59c97e/verification-uk-greenhouse-gas-emissions-using-atmospheric-observations-annual-report-2021.pdf.

McGillen, M. R., Z. T. P. Fried, M. A. H. Khan, K. T. Kuwata, C. M. Martin, S. O'Doherty, F. Pecere, D. E. Shallcross, K. M. Stanley, and K. Zhang, Ozonolysis can produce long-lived greenhouse gases from commercial refrigerants, *Proc. National Acad. Sci.*, *120*(51), e2312714120 (2023) doi:10.1073/pnas.2312714120.

Montzka, S. A., G. J. M. Velders, (Lead Authors), P.B. Krummel, J. Mühle, V.L. Orkin, S. Park, N. Shah, and H. Walter-Terrinoni, Hydrofluorocarbons (HFCs), Chapter 2 in: Scientific Assessment of Ozone Depletion: 2018, Global Ozone Research and Monitoring, World Meteorological Organization, Geneva, Switzerland (2018).

Montzka, S.A., G.S. Dutton, P. Yu, E. Ray, R.W. Portmann, J.S. Daniel, L. Kuijpers, B.D. Hall, D. Mondeel, C. Siso, J.D. Nance, M. Rigby, A.J. Manning, L. Hu, F. Moore, B.R. Miller, and J.W. Elkins, An unexpected and persistent increase in global emissions of ozone-depleting CFC-11, *Nature*, *557*, 413–417 (2018) doi:10.1038/s41586-018-0106-2.

Nilsson, E. J. K., O. J. Nielsen, M. S. Johnson, M. D. Hurley, and T. J. Wallington, Atmospheric chemistry of *cis*-CF_3CH=CHF: Kinetics of reactions with OH radicals and O_3 and products of OH radical initiated oxidation, *Chem. Phys. Lett.*, *473*, 233 (2009) doi:10.1016/j.cplett.2009.03.076.

NIST Gas Phase Kinetic Database, (2024), https://kinetics.nist.gov.

Østerstrøm, F. F., S. Thirstrup Andersen, T. I. Sølling, O. J. Nielsen, and M. P. Sulbaek Andersen, Atmospheric chemistry of Z- and E-CF_3CH=$CHCF_3$, *Phys. Chem. Chem. Phys*., *19*, 735-750 (2017) doi:10.1039/c6cp07234h.

Papanastasiou, D. K., A. Beltrone, P. Marshall, and J. B. Burkholder, Global warming potential estimates for the C_1-C_3 hydrochlorofluorocarbons (HCFCs) included in the Kigali Amendment to the Montreal Protocol, *Atmos. Chem. Phys.*, *18* (2018) 6317-6330, doi:10.5194/acp-18-6317-2018.

Park, H., J. Kim, H. Choi, S. Geum, Y. Kim, R.L. Thompson, J. Mühle, P.K. Salameh, C.M. Harth, K.M. Stanley, S. O'Doherty, P.J. Fraser, P.G. Simmonds, P.B. Krummel, R.F. Weiss, R.G. Prinn, and S. Park, A rise in HFC-23 emissions from eastern Asia since 2015, *Atmos. Chem. Phys.*, 23, 9401–9411 (2023) https://doi.org/10.5194/acp-23-9401-2023.

Pérez-Peña, M. P., J. A. Fisher, C. Hansen, and S. H. Kable, Assessing the atmospheric fate of trifluoroacetaldehyde (CF_3CHO) and its potential as a new source of fluoroform (HFC-23) using the AtChem2 box model, *Environ. Sci.: Atmos.*, *3*, 1767-1777 (2023) doi:10.1039/d3ea00120b.

Prinn, R.G., R.F. Weis, J. Arduini, T. Arnold, H.L. DeWitt, P.J. Fraser, A.L. Ganesan, J. Gasore, C.M. Harth, O. Hermansen, J. Kim, P.B. Krummel, S. Li, Z.M. Loh, C.R. Lunder, M. Maione, A.J. Manning, B.R. Miller, B. Mitrevski, J. Mühle, S. O'Doherty, S. Park, S. Reimann, M. Rigby, T. Saito, P.K. Salameh, R. Schmidt, P.G. Simmonds, L.P. Steele, M.K. Vollmer, R.H. Wang, B. Yao, Y. Yokouchi, D. Young, and L. Zhou, History of chemically and radiatively important atmospheric gases from the Advanced Global Atmospheric Gases Experiment (AGAGE), *Earth Syst. Sci. Data*, *10*, 985–1018 (2018) https://doi.org/10.5194/essd-10-985-2018.

Pu, J., H. Xu, B. Yao, Y. Yu, Y. Jiang, Q. Ma, and L. Chen, Estimate of hydrofluorocarbon emissions for 2012–16 in the Yangtze River Delta, *China, Adv. Atmos. Sci.*, *37*, 576–585 (2020).

Rigby, M., S. Park, T. Saito, *et al.* Increase in CFC-11 emissions from eastern China based on atmospheric observations. *Nature 569*, 546–550 (2019) https://doi.org/10.1038/s41586-019-1193-4.

Rust, D., M.K. Vollmer, S. Henne A. Frumau, P. van den Bulk, A. Hensen, K.M. Stanley, R. Zenobi, L. Emmenegger, and S. Reimann, Effective realization of abatement measures can reduce HFC-23 emissions. *Nature 633*, 96-100 (2024) https://doi.org/10.1038/s41586-024-07833-y.

Salierno, G. (2024), On the chemical pathways influencing the effective global warming potential of commercial hydrofluoroolefin gases, *ChemSusChem*, *e202400280*, doi:10.1002/cssc.202400280.

Schmidt, M., P. Bernath, C. Boone, M. Lecours, and J. Steffen, Trends in atmospheric composition between 2004–2023 using version 5 ACE-FTS data. *J. Quant. Spect. Rad. Trans.*, *325*, 1-24, Article 109088 (2024) https://doi.org/10.1016/j.jqsrt.2024.109088.

Simmonds, P. G., M. Rigby, A. McCulloch, M.K. Vollmer, S. Henne, J. Mühle, S. O'Doherty, A.J. Manning, P.B. Krummel, P.J. Fraser, D. Young, R.F. Weiss, P.K. Salameh, C.M. Harth, S. Reimann, C.M. Trudinger, L.P. Steele, R.H.J. Wang, D.J. Ivy, R.G. Prinn, B. Mitrevski, and D.M. Etheridge, Recent increases in the atmospheric growth rate and emissions of HFC-23 (CHF_3) and the link to HCFC-22 ($CHClF_2$) production, *Atmos. Chem. Phys*., *18*, 4153–4169 (2018) https://doi.org/10.5194/acp-18-4153-2018.

Stanley, K.M., D. Say, J. Mühle, C.M. Harth, P.B. Krummel, D. Young, S.J. O'Doherty, P.K. Salameh, P.G. Simmonds, R.F. Weiss, R.G. Prinn, P.J. Fraser, and M. Rigby, Increase in global emissions of HFC-23 despite near-total expected reductions. *Nat. Commun. 11*, 397 (2020) https://doi.org/10.1038/s41467-019-13899-4.

Sulbaek Andersen, M. P., and O. J. Nielsen, Tropospheric photolysis of CF_3CHO, *Atmos. Environ.*, *272*, 118935 (2022) doi:10.1016/j.atmosenv.2021.118935.

Sulbaek Andersen, M. P., S. Madronich, J.M. Ohide, M. Frausig, O.J. Nielsen, Photolysis of CF_3CHO at 254 nm and potential contribution to the atmospheric abundance of HFC-23. *Atmos. Environ*., *314*:120087 (2023) doi:10.1016/j.atmosenv.2023.120087.

Takeda, M., H. Nakajima, I. Murata, T. Nagahama, I. Morino, G.C. Toon, R.F. Weiss, J. Mühle, P.B. Krummel, P.J. Fraser, and H.-J. Wang, First ground-based Fourier transform infrared (FTIR) spectrometer observations of HFC-23 at Rikubetsu, Japan, and Syowa Station, Antarctica, *Atmos. Meas. Tech*., *14*, 5955–5976 (2021) https://doi.org/10.5194/amt-14-5955-2021.

TEAP (Technology and Economic Assessment Panel), Report of the Technology and Economic Assessment Panel, Volume 6: Response to Decision XXXIV/7: Strengthening Institutional Processes with Respect to Information on HFC-23 By-Product Emissions (2023b).

TEAP (Technology and Economic Assessment Panel), Report of the Technology and Economic Assessment Panel, Volume 5: Response to Decision XXXV/7: Emissions of HFC-23 (2024).

TEAP (Technology and Economic Assessment Panel), Report of the Technology and Economic Assessment Panel, Volume 6: Assessment of the funding requirement for the replenishment of the Multilateral Fund for the period 2021-2023, UNEP Ozone Secretariat, Nairobi; ISBN: 978-9966-076-93-9 (2021).

TEAP (Technology and Economic Assessment Panel), Report of the Technology and Economic Assessment Panel, Volume 3: Assessment of the Funding Requirement for the Replenishment of the Multilateral Fund for the Period 2024-2026; UNEP Ozone Secretariat, Nairobi; ISBN: 978-9914-733-88-4 (2023a).

UNTC (United Nations Treaty Collection), Amendment to the Montreal Protocol on Substances that Deplete the Ozone Layer, No. 26369, XXVii, 2.f. https://treaties.un.org/doc/Publication/MTDSG/Volume%20II/Chapter%20XXVII/XXVII-2-f.en.pdf (2019).

UNEP (United Nations Environment Programme), Executive Committee of the Multilateral Fund for the Implementation of the Montreal Protocol, Country Programme data and prospects for compliance, 74th meeting, UNEP/OzL.Pro/ExCom/74/11, United Nations Environment Programme, Montreal, Canada, [available at: http://www.multilateralfund.org/74/English/1/7411.pdf] (2015).

UNEP (United Nations Environment Programme), Executive Committee of the Multilateral Fund for the Implementation of the Montreal Protocol, Cost-effective Chapter 2 151 Options for Controlling HFC-23 By-product Emissions (Decision 81/68(e)), United Nations Environment Programme, Montreal, Canada, [available at: http://multilateralfund.org/82/English/1/8268.pdf] (2018a).

UNEP (United Nations Environment Programme), Executive Committee of the Multilateral Fund for the Implementation of the Montreal Protocol, Corrigendum: Cost-effective Options for Controlling HFC-23

By-product Emissions (Decision 81/68(e)), United Nations Environment Programme, Montreal, Canada (2018b) [available at: http://multilateralfund.org/82/English/1/8268c1.pdf].

UNEP (United Nations Environment Programme), Executive Committee of the Multilateral Fund for the Implementation of the Montreal Protocol, Report of the sub-group on production sector (reissued), United Nations Environment Programme, Montreal, Canada (2020) http://multilateralfund.org/84/English/1/8474ri.pdf.

UNEP (United Nations Environment Programme), Executive Committee of the Multilateral Fund for the Implementation of the Montreal Protocol, Report on the subgroup on the production sector, United Nations Environment Programme, Montreal, Canada (2022a) [available at: http://www.multilateralfund.org/91/Agenda%20item%2016%20Report%20of%20the%20Subgroup%20on%20the%20Produ/1/9171ri.pdf].

UNEP (United Nations Environment Programme), Executive Committee of the Multilateral Fund for the Implementation of the Montreal Protocol, Report of part II of the Eighty-ninth meeting of the Executive committee, United Nations Environment Programme, Montreal, Canada (2022b) [available at: http://multilateralfund.org/89/Report%20of%20the%20eightyeighth%20meeting%20of%20the%20Executiv/1/8916.pdf].

UNEP (United Nations Environment Programme) Ozone Secretariat, Country Data, Additional Reported Information, HFC-23 Emissions (2024) [available at: https://ozone.unep.org/additional-reported-information].

UNFCCC (United Nations Framework Convention on Climate Change), *United Kingdom. 2023 National Inventory Report (NIR), Annex 6* (2023) [available at: https://unfccc.int/documents/627789].

UNFCCC (United Nations Framework Convention on Climate Change), *Australia. 2024 National Inventory Document (NIR), Annex V* (2024) [available at: https://unfccc.int/documents/637882].

UNFCCC (United Nations Framework Convention on Climate Change)*, Greenhouse Gas Inventory Data - Flexible Queries Annex 1 Parties;* (2024a) https://di.unfccc.int/flex_annex1.

UNFCCC (United Nations Framework Convention on Climate Change)*, Greenhouse Gas Inventory Data - Flexible Queries non Annex 1 Parties*; (2024b) https://di.unfccc.int/flex_non_annex1.

Vollmer, M. K., S. Reimann, M. Hill, and D. Brunner, First observations of the fourth generation synthetic halocarbons HFC-1234yf, HFC-1234ze(E), and HCFC-1233zd(E) in the atmosphere, *Environ. Sci. Technol., 49* (5), 2703-2708 (2015) doi:10.1021/es505123x.

Wallington, T. J., W. F. Schneider, D. R. Worsnop, O. J. Nielsen, J. Sehested, W. J. DeBruyn, and J. A. Shorter, The environmental impact of CFC replacements- HFC and HCFCs, *Environ. Sci. Technol.*, *28*(7), 320-326 (1994) doi:10.1021/es00056a714.

Wang, Y., Z. Wang, M. Sun, J. Guo, and J. Zhang, Emissions, degradation and impact of HFO-1234ze from China PU foam industry, *Sci. Total Environ.*, *780*, 146631 (2021) doi:10.1016/j.scitotenv.2021.146631.

Wang, Y., M. An, L. Western, R.G. Prinn, J. Hu, X. Zhao, M. Rigby, J. Muhle, M.K. Vollmer, R.F. Weiss, and B. Yao, Rising perfluorocyclobutane (PFC-318, c-C_4F_8) emissions in China from 2011 to 2020 inferred from atmospheric observations. *Environ. Sci. Technol.*, *58,* 26, 11606-11614 (2024) https://doi.org/10.1021/acs.est.3c10325.

Yao, B., M. K. Vollmer, L. X. Zhou, S. Henne, S. Reimann, P. C. Li, A. Wenger, and M. Hill, In-situ measurements of atmospheric hydrofluorocarbons (HFCs) and perfluorocarbons (PFCs) at the Shangdianzi regional background station, China, *Atmos. Chem. Phys., 12*, 10181–10193 (2012) www.atmos-chem-phys.net/12/10181/2012/.

Yi, L, M. An, H. Yu, Z. Ma, L. Xu, S. O'Doherty, M. Rigby, L. M. Western, A. L. Ganesan, L. Zhou, Q. Shi, Y. Hu, B. Yao, W. Xu, J. Hu, In Situ observations of halogenated gases at the Shangdianzi background station and emission estimates for Northern China, *Environ. Sci. Technol.*, *57*, 18, 7217–7229 (2023) https://doi.org/10.1021/acs.est.3c00695.